Impulse Propagation at the Septal and Commissural Junctions of Crayfish Lateral Giant Axons

A. WATANABE and H. GRUNDFEST

From the Department of Neurology, College of Physicians and Surgeons, Columbia University, New York, and the Marine Biological Laboratory, Woods Hole. Dr. Watanabe's present address is Department of Physiology, Tokyo Medical and Dental University

ABSTRACT Transmission across the septal junctions of the segmented giant axons of crayfish is accounted for quantitatively by a simple equivalent circuit. The septal membranes are passive, resistive components and transmission is ephaptic, by the electrotonic spread of the action current of the pre-septal spike. The electrotonic spread appears as a septal potential, considerably smaller than the pre-septal spike, but usually still large enough to initiate a new spike in the post-septal segments. The septal membranes do not exhibit rectification, at least over a range of ± 25 mv polarization and this accounts for their capacity for bidirectional transmission. The commissural branches, which are put forth by each lateral axon, make functional connections between the two axons. Transmission across these junctions can also be bidirectional and is probably also ephaptic. Under various conditions, the ladder-like network of cross-connections formed by the commissural junctions can give rise to circus propagation of impulses from one axon to the other. This can give rise to reverberatory activity of both axons at frequencies as high as 400/sec.

INTRODUCTION

The discovery of segmented septate giant axons in crayfish (55) and earthworm (76) raised a new type of problem regarding the nature of transmissional processes. Like other giant axons of invertebrates (*cf.* reference 86) the septate nerves arise by fusion of small fibers of many cells. In the septate axons, however, the fused process originates from a segmental group of cells and the fiber produced in each segment abuts its neighbors in the segments fore and aft. Although in some forms the axons of several segments may fuse, in crayfish the axons of the individual segments are separated by membranes or septa. The membranes have been studied with the electron microscope recently by Hama (48). Unlike the septal surfaces of earthworms (47, but *cf.* reference 54) those of the crayfish are covered by Schwann cells and connective

tissue. They form a layer about 2 μ thick in the crayfish. There are occasional patches or "windows," however, where the two axonal membranes come together to lie only about 100 A apart.

It was inferred (55, 76) that the segmented giant axons, which run the length of the animal, were through conducting systems of considerable importance to nervous functioning. The septa appeared to be so different in structure from synapses that Johnson (55) thought they also represented a different mode of transmissional activity. Stough (76) and Holmes (53), however, held that the septal membranes formed synaptic structures.

Electrophysiological data demonstrated that the segmented axons conducted impulses in both directions in earthworm (14, 24, 74) and in crayfish (85). These findings emphasized the difference between the bidirectional septa and unidirectional synapses, and the former were termed "unpolarized synapses" (*cf.* reference 15). Wiersma (85) noted that transmissional delay at the septa was brief, whereas a significant delay ranging up to several milliseconds occurs in synaptic transmission (21, 23, 36).

Previous studies in this laboratory with microelectrode recordings from the septate giant axons of earthworm and crayfish were primarily concerned with their spikes and with the role of the postsynaptic potentials (p.s.p.'s) that are recorded from these axons (57–59). Such evidence as bore on transmission across the septa indicated that it was ephaptic (36), the action current from an excited segment apparently spreading electrotonically across the septum, as it also does along single nerve or muscle fibers. Since a response of the neighboring segment thus is evoked by electrical local circuit excitation, ephaptic transmission thereby differs fundamentally from synaptic transmission, which involves electrically inexcitable postsynaptic electrogenesis (34, 36).

The experiments described in the present paper were designed to study the transmissional process across the septal membranes of the crayfish axons in sufficient detail so as to provide data on specific physical and physiological properties of the membranes. The information obtained in the course of this study shows that transmission is, indeed, ephaptic. The data account in quantitative terms for the fact that transmission across the septal membrane is bidirectional, whereas ephaptic transmission from the cord lateral giant axon to the root motor giant fiber of the crayfish is unidirectional (29). Another bidirectional, and probably ephaptic system, was also found to occur at the commissural junctions between the homologous segments of the two lateral giant fibers. Thus, impulses can propagate not only from segment to segment within each axon, but can also travel from one axon to the other along the ladder of cross-couplings made by the commissural branches. These connections can give rise to reverberatory repetitive activity of both lateral axons at a high frequency.

METHODS

Relatively large crayfish were selected for these experiments. After removing the dorsal exoskeleton and the muscles overlying the ventral nerve cord the latter was carefully dissected free in the stretch from the middle of the thorax to the 6th abdominal ganglion. On its removal from the animal the nerve cord was further cleared of muscle fragments and loose connective tissue under a binocular microscope. It was then placed in a trough on a lucite plate. Sunk into the floor of the trough were several pairs of fine chlorided silver wires for stimulating and recording. The nerve cord was fixed at both ends and was also held down by two partitions across the trough formed out of soft vaseline. Thus, the chamber was divided into three well insulated parts. Stimulation and recording with the external electrodes could take place in each part or across the partition with minimal spread of current and with relatively little shunting, although the tissue was covered with crayfish saline (79).

The 2nd abdominal ganglion was usually chosen for penetration of axons with microelectrodes. The axons at the level of this ganglion were larger than in the more caudal parts, while the ganglion was still small enough to permit good transillumination. The ganglion was placed in the middle portion of the trough. Part of the connective tissue was removed after the nerve cord was fixed in the holder.

The four giant axons of the nerve cord were visualized in darkfield illumination (Fig. 1). Only the two lateral fibers are septate and segmental in origin. The septa run diagonally forward from the mesial aspects of the axons, so that the apposition of two segments occurs over a considerable length of the axon. Some septa could be observed stretching for more than 800 μ. Electrophysiological evidence also showed that the segments overlap by as much as 500 μ. Thus, the inclination of the septa to the long axis of the axon was much less than 45° (85). However, the angle probably depended upon the degree of stretch applied to the nerve cord when it was fixed in its holder. A commissural branch (55) runs medially from the caudad base of each segment. The branches from the two lateral giant axons meet in the midline.

Glass microcapillary electrodes filled with 3 M KCl (56, 68) were employed for intracellular recording and for applying polarizing currents intracellularly. As many as four microelectrodes were inserted into a single axon in some experiments. In others, both lateral giant axons were impaled for simultaneous registration of their activity. A few comparisons were also made between the lateral and medial giant axons and on occasion some smaller axons of the nerve cord were impaled without visual control.

The manipulators, stimulators, amplifying and recording equipment were standard for the laboratory and have been described elsewhere (2, 9, 33). Since the spike of the crayfish giant axons is very brief and has a steep rise (*cf.* Fig. 2), accurate recording of the amplitude and form depended upon careful adjustment of the neutralizing capacity of the input amplifiers. Those in present use could be adjusted to have a rise time of 10 to 15 μsec. with the high resistance (10 to 25 megohm) microelectrodes employed in the present work. The frequency response of the system was monitored continuously by injecting a square pulse calibration at the beginning of each sweep,

as shown in Fig. 3*D*. For the experiments in which currents were applied to the preparation intracellularly, each microelectrode recording was differential against an external electrode so as to eliminate common mode interference.

The experiments were carried out at room temperatures ranging from 18 to 24°C. The crayfish were obtained at the different seasons from suppliers in Louisiana and

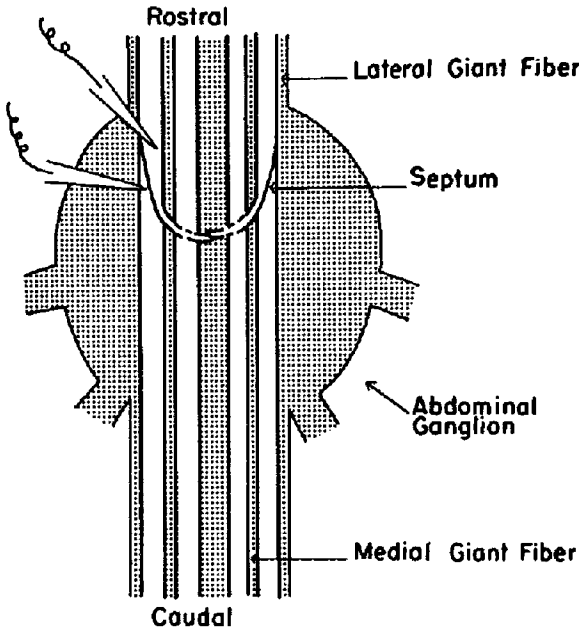

FIGURE 1. The giant fiber system of crayfish shown diagrammatically as it appears in the transilluminated preparation. The two lateral giant fibers (about 100 μ diameter) are distinguished from the pair of medial axons by the presence of septa which occur at each of the ganglia and which divide the lateral giant axons into autonomous segmental units. The commissural branches connecting the two lateral giant axons are rarely seen in intact preparations and never in their entirety. They are drawn after Johnson (55), and on the basis of the electrophysiological data. Microelectrodes are drawn inserted at each side of the septum in the left lateral giant axon.

Wisconsin. Some of the animals were identified as *Procambarus clarkii*, but others of unidentified species were also used. However, no consistent differences were observed between batches from different localities. The work covered a period which included two summers (1959 and 1960), but no seasonal differences were observed.

RESULTS

A. *The Electrogenic System*

THE RESTING POTENTIAL. The resting potentials ranged from 70 to 90 mv, inside negative. These values are similar to those found in other studies

on crayfish axons (22, 29, 44, 57). It is likely that the smaller values frequently were from impaired fibers. Axons with the lower resting potentials had smaller spikes and sometimes conduction into a segment that had a low resting potential was blocked. Penetration of the giant axons is hampered by their thick connective tissue sheaths. It may therefore be expected that penetrations often caused damage.

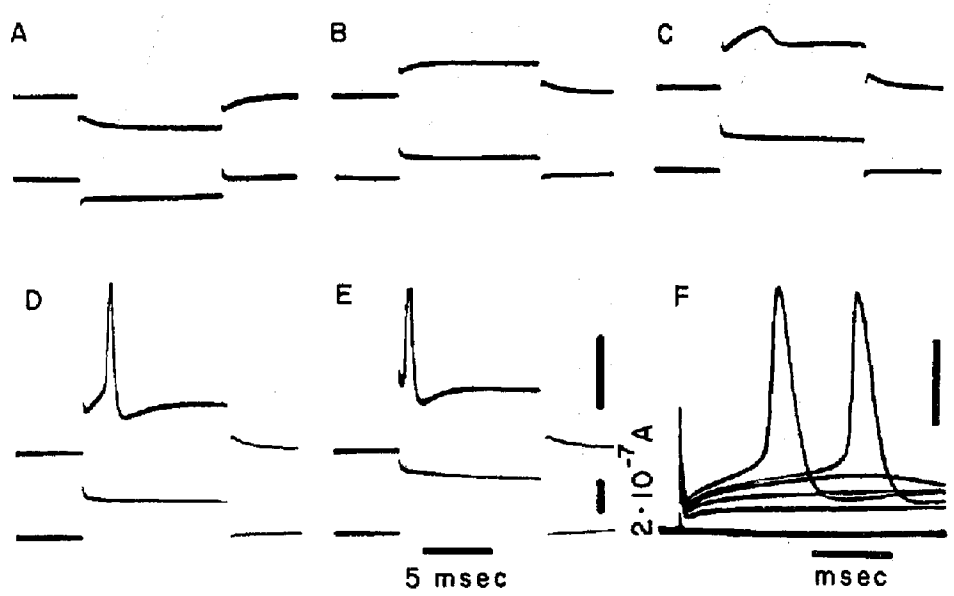

FIGURE 2. Responses of a lateral giant axon to intracellularly applied currents. *A–E*, from one preparation. Current monitoring on lower trace, upward deflection denotes outward, depolarizing current. *A*, *B*, weak hyperpolarizing and depolarizing currents. *C*, a local response was evoked by a stronger depolarizing current. *D*, *E*, spikes evoked by stronger stimuli. *F*, another fiber, showing superimposed registration of five traces with progressively increasing depolarizing currents. Note the undershoot following spike elicited during sustained depolarization. Calibrations 50 mv in this and in subsequent figures, unless otherwise specified.

RESPONSES TO INTRACELLULAR STIMULI A graded local response was evoked by depolarizations exceeding about 15 mv (Fig. 2*C*; *cf.* also Figs. 18 and 20). The directly evoked spikes arose at critical firing levels ranging between 30 and 50 mv in different axons. They had a maximum rate of rise of up to 1200 v/sec. and attained a peak of up to 150 mv in axons which had large resting potentials. The spikes were brief, about 200 to 500 μsec., measured at their half-amplitude level. When they were evoked by sustained depolarization the spikes had a marked undershoot. The latter was never seen when the spikes were evoked by brief stimuli or when a response arose by propagation into the segment. Instead, there was then an after-depolarization

(Figs. 3 to 7). Except for the special circumstances of reverberatory cross-excitation between the two lateral giant axons, which will be described below, long lasting depolarizing stimuli usually evoked only a single spike (*cf.* Fig. 18*B*).

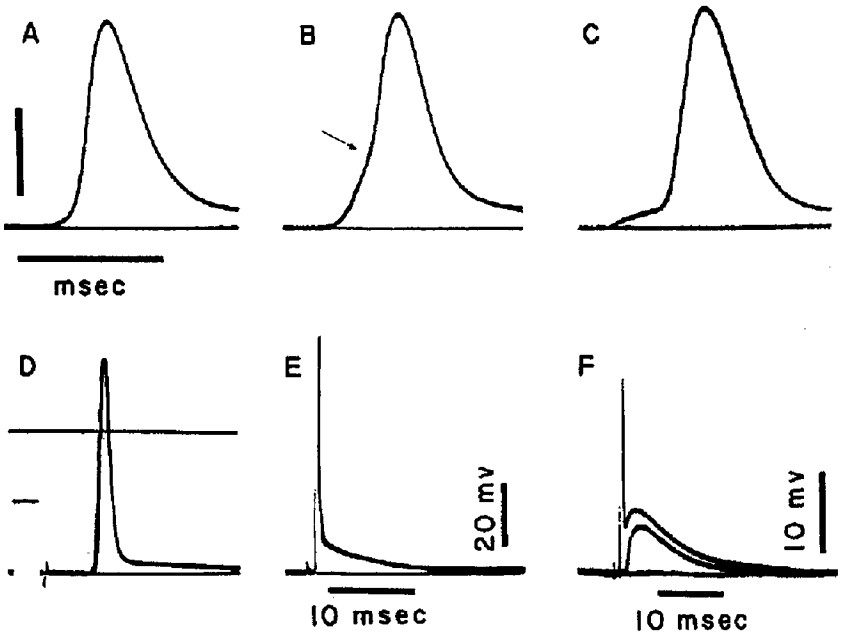

FIGURE 3. The action potentials of lateral giant axons evoked by stimulating the nerve cord. *A*, "pre-septal" spike recorded before transmission across the septum. The spike ends with a depolarizing after-potential. *B*, the "post-septal" spike of the same axon, recorded after transmission across the septum. The slowly rising initial portion is the "septal potential" by which the spike of the post-segment was initiated. Arrow shows the inflection at about 45 mv depolarization produced by the septal potential. The opposite lateral giant axon was destroyed for these records. *C*, another preparation in which the pre-septal spike was initiated by excitation from the opposite lateral giant axon. The small initial deflection is the electrotonic potential of the larger depolarization at the distant junctional site of the commissural branches. *D*, *E*, the depolarizing after-potential is seen at slower recording speeds and at different amplifications. Each record is of two superimposed sweeps with and without a response. The zero reference of the recording is shown as the upper trace in *D*. A 50 mv, 1 msec. calibrating pulse to check the neutralization of the input capacity is shown at the beginning of the trace in this record. *F*, three superimposed records, respectively, without a stimulus; with a weak stimulus which evoked only a postsynaptic potential; and with a stronger stimulus which evoked the conducted spike.

SPIKES AND PREPOTENTIALS ASSOCIATED WITH PROPAGATED RESPONSES

The spikes evoked in a segment on stimulating the nerve cord some distance away differed in form depending on the relation between the origin of the spike and the recording site. When the recording microelectrode was distant

from the septum, the spikes had a smooth configuration, as did the directly evoked spikes, no matter whether the propagation into the segment was rostrad or caudad. The same form was also obtained when the microelectrode

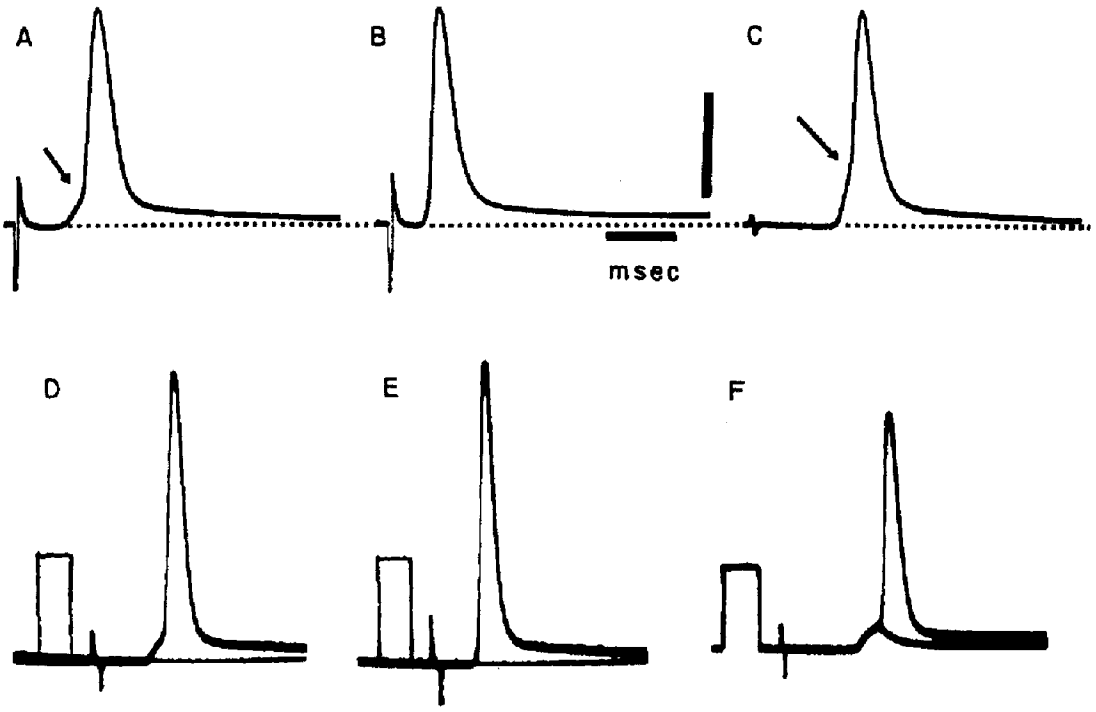

FIGURE 4. Responses evoked in lateral giant axon by commissural transmission and by propagation within the axon in either direction. *A*, response elicited pre-septally in the right axon by a weak stimulus to the rostral nerve cord had a small prepotential (as in Fig. 3*C*) associated with transmission across commissural branches of the activity initiated in the left axon. *B*, a stronger stimulus excited the right axon directly. The latency was shortened by about 0.7 msec. and the spike caused by local circuit excitation arose abruptly as in Fig. 3*A*. *C*, on stimulating the caudal nerve cord the spike rose out of a septal potential, as in Fig. 3*B*. Note the different amplitudes of the two prepotentials. *D* and *E*, another experiment, records as in *A* and *B*. *F*, another preparation. One of the two stimulations did not evoke a transcommissural spike. Calibrating pulses 50 mv and 1 msec.

was close to the septum and the spike was recorded before traversing the septum (*i.e.*, it was "pre-septal"; Fig. 3*A*).

When the spike was "post-septal," *i.e.* recorded just after passage across the septum, its rising phase had an initial slow part, with the steeper phase arising from a more or less distinct notch (*B*). As will be described below, the initial "septal potential" is responsible for transmission across the septum. A smaller prepotential, usually no more than about 10 mv in amplitude,

sometimes appeared (*C*) when the recording microelectrode was just rostrad to the septum. This potential is associated with transmission across the commissural branches of the activity initiated at a lower threshold in the opposite lateral giant axon (Fig. 4*A*). When both axons were excited by a stronger stimulus, the spike at the recording site arose earlier, by conduction within the axon itself (Fig. 4*B*). The conduction velocity ranged between 7.6 and 13.8 m/sec. (mean 10.6 ± 1.1 m/sec.). These values agree with earlier data (85).

AFTER-POTENTIAL At least part of the after-depolarization which succeeded the propagated spike was an after-potential lasting about 20 msec. (Fig. 3*D*, *E*). This potential usually developed smoothly out of the falling phase of the spike, but occasionally a peak of some 5 to 10 mv was produced

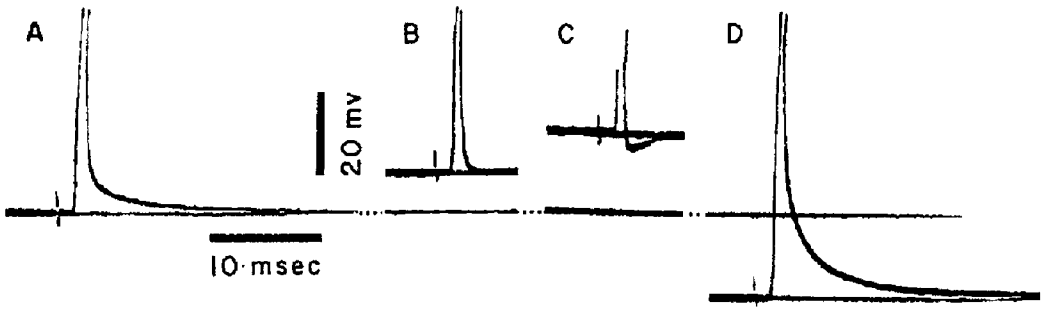

FIGURE 5. Changes in after-potential with changes in membrane polarization. The initial resting potential is shown in all records. *A*, response elicited with the axon at its resting potential. On depolarizing the axon with an intracellularly applied current the after-potential was abolished (*B*) and reversed in sign (*C*). When the axon was hyperpolarized (*D*) the after-potential increased.

by a small dip of the falling phase. The depolarizing ("negative") after-potential decreased in amplitude when the segment was depolarized by applied currents, and on depolarizations of somewhat over 10 mv, the sign of the after-potential reversed (Fig. 5*B*, *C*) so that it became an undershoot (*cf.* also Fig. 2*D*, *F*). The amplitude and duration of the after-potential increased when the axon was hyperpolarized (Fig. 5*D*). The early dip, if it was present, then disappeared. Thus, the after-potential is probably generated by increased conductance for K^+ or Cl^- (39). Presumably the after-potential is caused by the same process which is manifested as rectification in the axons (*cf.* Figs. 11 and 13). A similar after-potential, but markedly smaller in amplitude, also follows the spikes of medial giant fibers.

P.S.P.'s Depolarization of another origin (Fig. 3*F*) was also often observed. It could be made to appear without the spike in either lateral axon by carefully grading the stimulus to the nerve cord. When, on increasing

the stimulus, a spike was evoked, it appeared earlier than the independent potential, indicating that the excitant pathway for the latter had a lower conduction velocity than did propagation in the lateral giant axon. These potentials, which are p.s.p.'s that probably develop on stimulation of smaller fibers, have been observed in the motor giant axons (30, 44) as well as in lateral giant axons of earthworm (59). Their occurrence in the crayfish lateral giant axons was described in earlier work from this laboratory (57, 58).

MEMBRANE CONSTANTS Electrical properties of three lateral axons are shown in Table I. These cable constants of the membranes (52, 64) were estimated from data obtained with intracellularly applied pulses (*cf.* reference

TABLE I

MEMBRANE CONSTANTS OF LATERAL GIANT AXONS

Fiber	d	λ	r_e $10^5\Omega$	r_i $10^5\Omega$/mm	r_m $10^5\Omega$/mm	R_i Ωcm	R_m $10^3\Omega cm^2$	τ_m	C_M
	μ	mm						msec.	$\mu f/cm^2$
I	100	2.81	1.74	1.22	9.84	94	3.1	1.9	0.61
II	100	3.36	1.56	0.97	10.5	75	3.3	1.2	0.35
III	100	1.73	1.13	1.32	3.92	102	1.2	0.98	0.79

d, diameter of axon; λ, length constant; r_e, effective resistance between current electrode and ground return; r_i, internal resistance of 1 mm of the axon; r_m, membrane resistance of 1 mm of axon; R_i and R_m, specific resistances of the axoplasm and membrane respectively; τ_m, C_M, membrane time constant and capacity, respectively.

27). However, because the lateral axons have septal divisions and commissural branches, the cable equations do not apply precisely. Further inaccuracy results from the considerable variation in the diameter of the axons, which could be observed even over a length of only a few millimeters, or within the limits of the calculated length constant.

B. *Septal Transmission*

COMMUTATIVE NATURE OF THE SEPTAL POTENTIAL As already noted, when two microelectrodes were inserted close together, but on opposite sides of the septum, the responses at the two sites differed, depending upon the direction of the impulse relative to the recording electrodes (Figs. 3 and 4). No matter in which direction the impulse was travelling the post-septal spike always developed with a slow initial phase and was therefore markedly delayed in transmission (Fig. 6). Under the conditions of the experiments, some damage was probably produced by the microelectrode penetrations and the rising phase of the post-septal spike usually had a marked notch.

In Fig. 6*A* the pre-septal spike was in the rostrad segment. The post-septal

response was recorded only 50 μ away in the caudad segment. The amplitudes and durations of the spikes differed sufficiently so that the reversed sequence in Fig. 6*B*, with the spike of the caudal segment preceding and produced by stimulating the caudal part of the nerve cord, is clearly evident. The critical depolarization for evoking the post-septal spike was nearly equal in the two

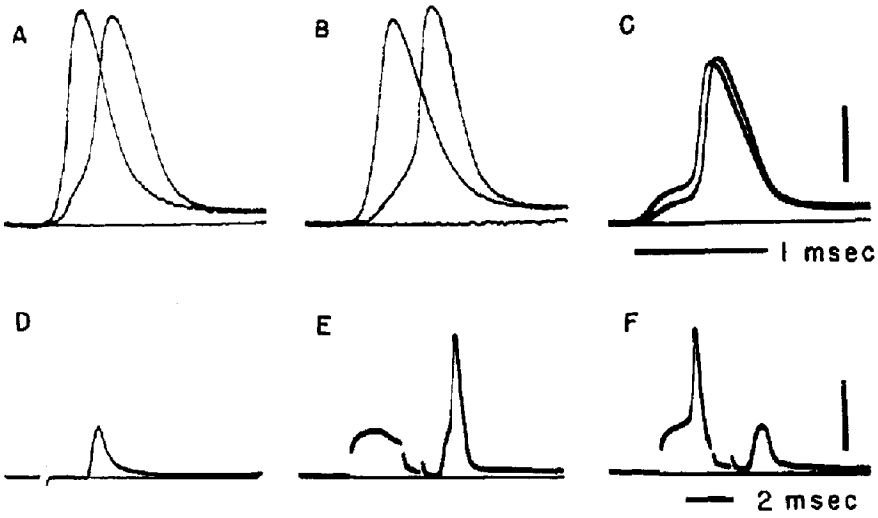

FIGURE 6. Septal transmission of lateral giant fibers. *A*, *B*, two microelectrodes were inserted, less than 50 μ apart but on either side of the septum. A stimulus was delivered to the rostral part of the nerve cord (*A*), and to the caudal (*B*). The spike of the rostrad segment was slightly the larger. Transmission across the septum in either direction involved a septal potential. Caudorostral delay was somewhat longer than in the reverse direction. *C*, another preparation. Two microelectrodes were inserted into the same segment, one close to the septum, the other 370 μ rostrad. The caudal part of the nerve cord was stimulated. The septal potential at the rostrad recording site was markedly diminished, the spike arising by propagation of the intrasegmentally originated local circuit. *D*, another preparation. A septal potential in a segment in which transmission had become blocked. *E*, *F*, another preparation. Stimulating current was applied through a microelectrode. The post-septal response evoked by a distant external stimulus was not affected by a prior subthreshold depolarizing stimulus (*E*), but transmission was blocked when a direct spike was evoked. The depolarization by the septal potential which remained was about the same in amplitude as the depolarization at which the direct spike was evoked.

cases, a finding which is in keeping with the fact that the critical firing level on intracellular depolarization (Fig. 2) was relatively constant in different segments in all the axons that were examined.

SEPTAL DELAYS The occurence not only of a septal delay, but also of a systematic difference, with delay for conduction toward the tail smaller than that in the opposite direction, was observed in most of the experiments in

which the matter was examined (Table II). In the experiment of Fig. 6 the two delays were 130 μsec. and 250 μsec. respectively, when measured at a level 50 mv positive to the resting potential. The difference may be seen to be associated with a more gradual rise in the beginning of the post-septal spike when the impulse was travelling toward the head (Fig. 6*B*). The septal delay was not due to conduction time along the axon; within the limits of

TABLE II

SEPTAL DELAYS IN 10 AXONS

Fiber	Distance between electrodes	Delay	
		Rostrocaudal conduction	Caudorostral conduction
	μ	μsec.	μsec.
I	25	50	160
II	50	70	120
III	50	210	220
IV	50	210	300
V	50	130	250
VI	100	40	140
VII	200	210	250
VIII	350	240	410
IX	370	210	180
X	−280	210	160

The potentials of fiber V are shown in Fig. 6*A* and *B*. In fiber X the electrode in the rostrad segment was 280 μ behind that in the caudad segment.

measurement on the living axon the diameter at the rostral and caudal ends is the same. The delays were not directly related to the distance apart of the two electrodes. In one case (fiber X of Table II) the pre-septal recording electrode was actually 280 μ behind the post-septal, advantage being taken in this experiment of a clearly visible stretch of oblique contact between the two segments.

SITE OF ORIGIN OF THE SEPTAL POTENTIAL The initial or "septal" phase of the post-septal response was frequently obscured by the rapidly rising spike, as in the three preparations of Table II in which rostrocaudal delay ranged between 40 and 70 μsec. When the delays were long, recording at two different sites in the post-septal segment showed that the septal component of the response diminished with distance (Fig. 6*C*). The simultaneously recorded spikes also differed at the two sites, but the one more distant from the septum was slightly the larger. Thus, while the spike arose regeneratively by sequential local circuit excitation within the segment, the initial septal component apparently occurred only at the septal region.

SPIKE INITIATION BY THE SEPTAL POTENTIAL Frequently, damage prevented initiation of a post-septal spike and the potential of the damaged

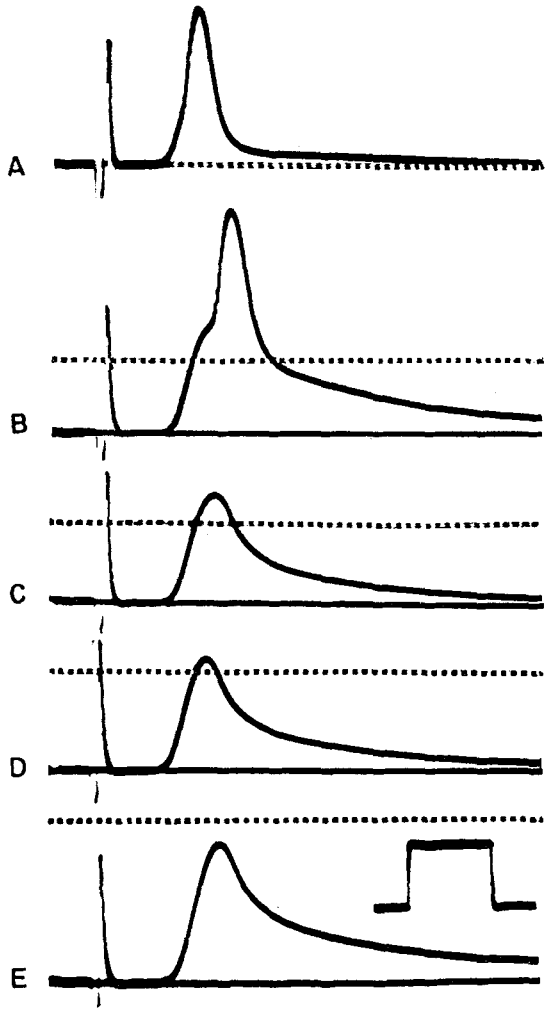

FIGURE 7. Changes in the post-septal response evoked by a stimulus to the nerve cord during hyperpolarization of the segment by an intracellularly applied current. The initial resting potential is shown by the broken line. *A*, before applying current. Transmission across the septum occurred with little delay. *B*, the delay was marked, and (*C*) the spike was abolished by small increases in the current. Note the increase in the after-potential following the hyperpolarized spike (*B*) and the persistence of a smaller septal after-potential when the spike was eliminated. Further hyperpolarization of the segment at first shortened and diminished the falling phase of the septal potential slightly (*D*), but the potential augmented when the segment was hyperpolarized still more strongly (*E*). Calibrating pulse 50 mv and 1 msec.

segment was only a septal potential (Fig. 6*D*). An indication that the septal potential is itself the excitant for the post-septal spike is also shown in Fig. 6. The transmitted spike arose at the same level of depolarization by the septal potential (*E*) as did a directly evoked spike from intracellularly applied

depolarization (*F*). In the latter case relative refractoriness in the directly excited segment resulted in failure of the post-septal spike to develop. The septal potential remained, its amplitude not significantly different from the critical level of depolarization from which the direct spike arose.

BLOCK OF SEPTAL TRANSMISSION BY HYPERPOLARIZING THE POST-SEPTAL SEGMENT When the post-septal segment was hyperpolarized (Fig. 7), the

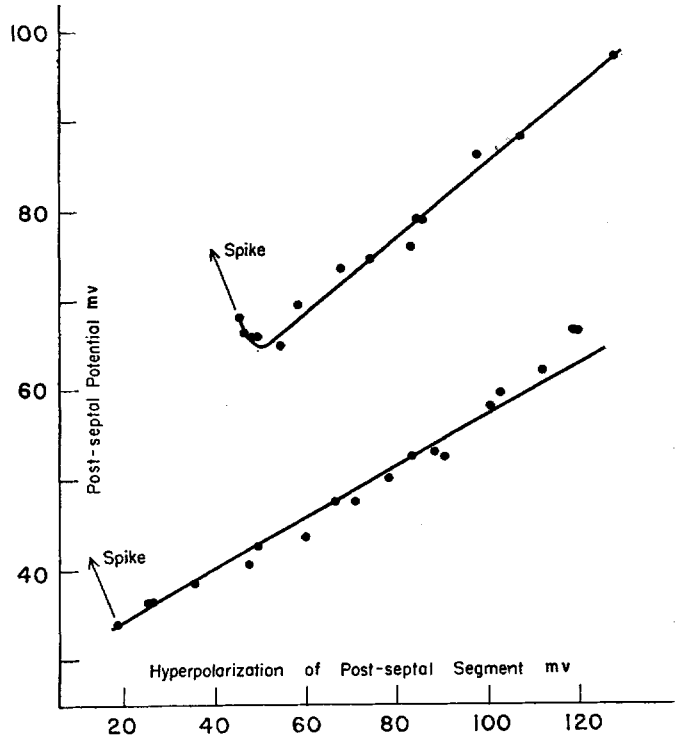

FIGURE 8. Changes in septal potential with hyperpolarization of the post-septal segment. Two preparations. The zero of abscissa is the resting potential of the axons and the potentials shown are negative. Note that the origins of the graphs are not shown. The regression lines of the two experiments crossed the abscissa at values only 4 mv apart, near + 100 mv.

spike was progressively delayed on the septal potential (*B*) and was eventually blocked (*C–E*). The remaining post-septal potential at first retained a component of local response (*C*). Production of a local response of the electrically excitable membrane by a depolarizing p.s.p. also occurs during relative refractoriness or by hyperpolarization of eel electroplaques (1) and other cells (36). The local response of the axon was eliminated by further hyperpolarization leaving a "pure" septal potential (*D*). However, with further increase of the hyperpolarization (*E*) the septal potential also increased in

amplitude as does a p.s.p. (36). The shape of the septal potential also appeared to resemble that of p.s.p.'s of many types of cells (23, 36). Its rise time was about 0.5 msec., but a longer lasting falling phase led to a total duration of about 5 msec. The relation between the septal potential and the membrane potential was approximately linear, with a slope of 0.3 to 0.4 (Fig. 8). Slopes of similar magnitude also occur in the case of p.s.p.'s of hyperpolarized cells (*cf.* references 40, 43).

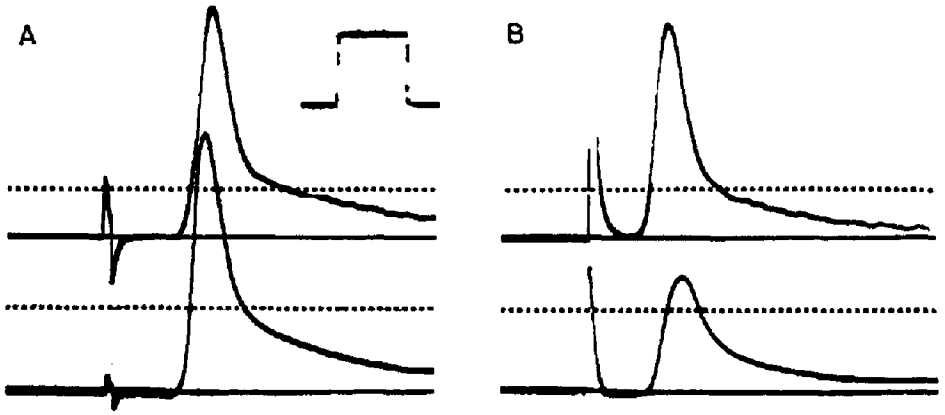

FIGURE 9. Effects of membrane hyperpolarization on pre- and post-septal potentials. Recording microelectrodes were inserted at each side of a septum. A microelectrode for polarizing currents was also inserted rostrad to the septum. The records show responses evoked by stimulating the rostral portion of the nerve cord (*A*) and the caudal (*B*) during application of a constant hyperpolarizing current. The initial resting potentials of the two segments are shown by broken lines. During the hyperpolarization of the rostrad segment there was also a smaller hyperpolarization of the caudad segment which is registered on the upper trace. *A*, the pre-septal spike of the strongly hyperpolarized rostrad segment was very large and initiated a spike in the caudad segment with a delay less than 100 μsec. measured between the two peaks. The post-septal spike was also large. *B*, stimulation of the caudal part of the nerve cord evoked a smaller spike in the caudad segment. Transmission across the septum was blocked, a septal potential remaining. Calibrating pulse 50 mv and 1 msec.

EFFECTS OF HYPERPOLARIZATION ON PRE- AND POST-SEPTAL SPIKES A constant hyperpolarizing current which was applied to the rostrad segment (Fig. 9) caused a smaller hyperpolarization in the caudad segment. When the rostral nerve cord was stimulated, the spike which invaded the strongly hyperpolarized pre-septal region was very large (*A*, *lower trace*). Transmission across the septum was also very effective. The latency of the post-septal spike (*upper trace*) was so brief that its origin on the septal potential was difficult to discern. Transmission in the opposite direction was blocked, however (*B*). Although the impulse invaded the pre-septal (now the caudad and the less strongly hyperpolarized) segment, its spike (*upper trace*) was

smaller than the pre-septal spike in the more strongly hyperpolarized segment. Excitability of the more hyperpolarized membrane of the rostrad segment was lower and the potential that resulted (*lower trace*) lacked a spike, although there may have been a component of local response on the septal potential. The post-septal potential started simultaneously with the large pre-septal spike in *A*. A slight delay which appears in *B* was probably due to the more

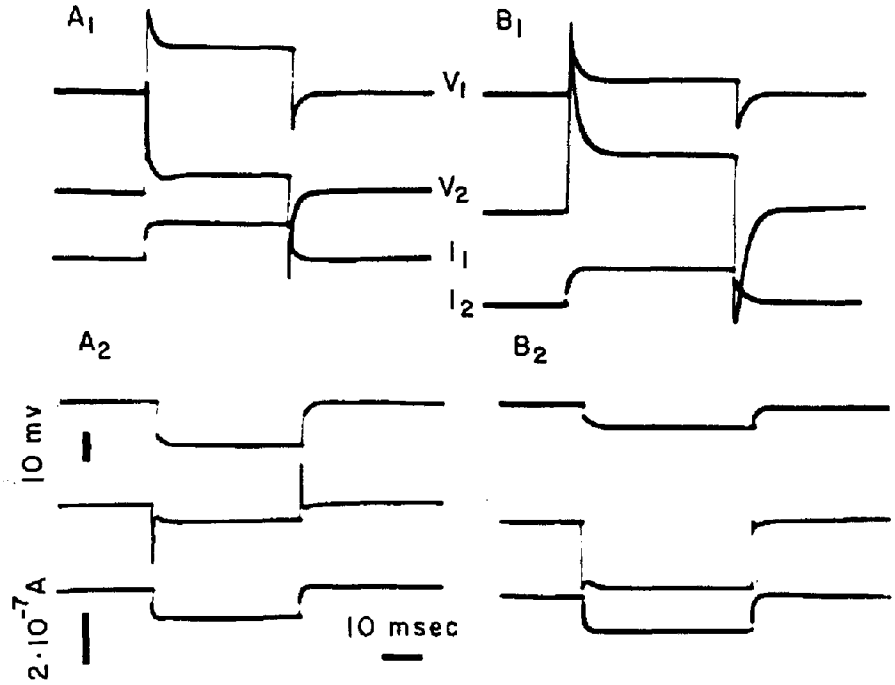

FIGURE 10. Electronic spread of potentials in either direction across the septum. Four electrodes were inserted close together, two on each side of the septum as in the diagram of Fig. 15. I_1, V_1 are the rostrad pair; I_2, V_2, are the caudad. A_1 and A_2, examples of the potentials recorded in the two segments for depolarizing and hyperpolarizing currents through I_1. B_1 and B_2 show similar records for currents through I_2.

slowly rising electrotonic potential produced by the smaller, less steeply rising spike. Synaptic latencies are usually about 0.5 msec. or more (36).

C. *Properties of Septal Membranes*

ELECTROTONIC SPREAD OF POTENTIAL ACROSS THE SEPTUM It is evident in Fig. 9 that hyperpolarization of one segment caused a considerable, though smaller, hyperpolarization of the nearby segment. This matter was investigated in detail in experiments such as those illustrated by Figs. 10 and 11. Two microelectrodes were inserted on each side of a septum. One of each pair was for applying current and the other for recording the membrane

potential. The three simultaneously recorded traces of sequences A_1 and A_2 show the effects of applying depolarizing (A_1) and hyperpolarizing (A_2) pulses through the electrode rostral to the septum. The upper trace in each case represents the "*cis*-septal" recording electrode; the second trace is of the "*trans*-septal" potential; while the lowest trace shows the applied current. In B_1 and B_2 the traces represent the same registration, but the polarizing

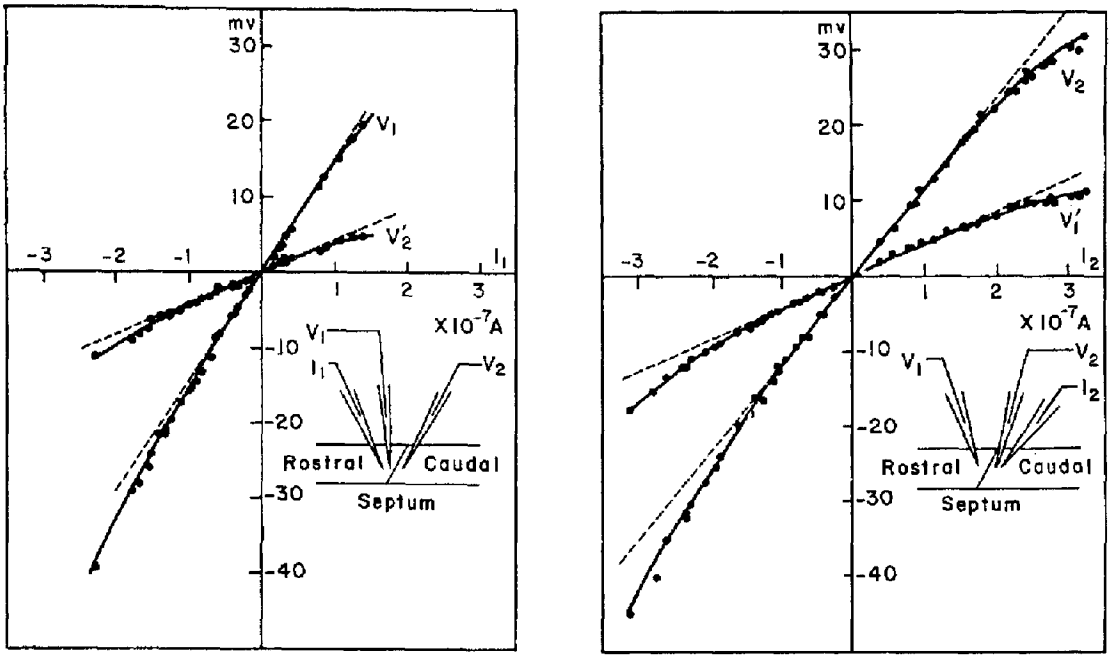

FIGURE 11. Current-voltage data obtained in a complete experiment from records like those of Fig. 10. Each inset diagram shows only the current electrode used for the relevant set of measurements. *Left*, I_1, varying, $I_2 = 0$; V_2' is the voltage of the trans-septal (caudad) segment. *Right*, I_2, varying, $I_1 = 0$; V_1' is the voltage of the trans-septal (rostrad) segment. Depolarizations in upper right quadrant. The broken lines show the gradients at the origins. Their values are given in Table III (fiber I). Further description in text.

currents were now applied through the electrode caudal to the septum, and the *cis*-septal potential was that on the second trace.

These records show that electrotonic spread occurred in both directions across the septum, for both depolarizing and hyperpolarizing currents. The *trans*-septal potential spreading across the septum was considerably attenuated in comparison with the *cis*-septal potential, the attenuation being of the order of two- to four-fold when the depolarizing current was small. Since the length constant of the axon is 2 to 3 mm (Table I) and the electrodes were grouped within a distance of about 100 μ, the attenuation could not have

been due to losses in a simple linear cable conductor system. Rather, the septum appears to act as a barrier of low electrical resistance.

The data obtained in experiments such as that of Fig. 10 are shown as a family of four voltage-current curves in Fig. 11. On the left are plotted the data obtained when the polarizing current was applied to the rostrad segment, and on the right are the symmetrical data for currents applied to the caudad segment. The ratio of the gradients around the origin of the two curves in each graph is the attenuation factor for small polarizing currents. In the experiment of Fig. 11 this value was 2.7 when the current was applied in the rostrad segment and 2.4 for current in the caudad segment. Thus, the septal membrane is essentially a symmetrical resistance for current flow in either

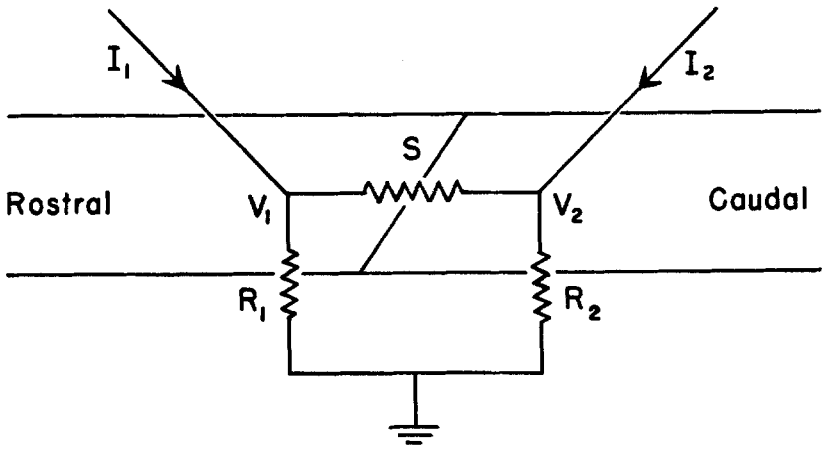

FIGURE 12. The equivalent circuit used for analyzing the properties of the septum and of the two segmental membranes, S, R_1 and R_2, respectively. The measurements of Figs. 10, 11, and 13 are indicated by I_1, V_1, I_2 and V_2.

direction. However, the voltage-current relation showed non-linearities which began with relatively small polarizations in both directions.

EQUIVALENT CIRCUIT OF SEPTATE AXONS In view of the symmetrical current distribution across the septum, it seemed feasible to represent the electrical properties of the axon by a relatively simple equivalent circuit (Fig. 12). For the steady state measurements of Figs. 10 and 11 capacitative elements could be neglected. The axonal membranes of the two segments are represented by resistances R_1 and R_2, coupled through the septal resistance S. This is essentially the same circuit as that used by Furshpan and Potter (29), except that the rectifier element of the coupling resistance at the lateral giant–motor giant junction could be omitted here.

RESISTANCE OF THE VARIOUS MEMBRANES Experiments like those of Fig. 11 may be analyzed in terms of the equivalent circuit of Fig. 12. I_1

divides into 2 branches: i_1 flowing through R_1 and causing the voltage drop V_1 and i_1', which causes the voltage V_2' on R_2. Similarly I_2 is subdivided into components i_2 and i_2'.

$$i_1 = \frac{(R_2 + S)}{\Sigma R} \cdot I_1 \tag{1}$$

$$i_1' = \frac{R_1}{\Sigma R} \cdot I_1 \tag{2}$$

$$i_2 = \frac{(R_1 + S)}{\Sigma R} \cdot I_2 \tag{3}$$

$$i_2' = \frac{R_2}{\Sigma R} \cdot I_2 \tag{4}$$

where

$$\Sigma R = R_1 + R_2 + S.$$

Accordingly

$$V_1 = R_1 i_1 = \frac{R_1(R_2 + S)}{\Sigma R} \cdot I_1 \tag{5}$$

$$V_2' = R_2 i_1' = \frac{R_1 R_2}{\Sigma R} \cdot I_1 \tag{6}$$

$$V_2 = R_2 i_2 = \frac{R_2(R_1 + S)}{\Sigma R} \cdot I_2 \tag{7}$$

$$V_1' = R_1 i_2' = \frac{R_1 R_2}{\Sigma R} \cdot I_2 \tag{8}$$

The gradients at the origins of the four curves of Fig. 11 are the differential coefficients of equations 5 to 8.

$$\frac{dV_1}{dI_1} = \frac{R_1(R_2 + S)}{\Sigma R} \tag{9}$$

$$\frac{dV_2'}{dI_1} = \frac{R_1 R_2}{\Sigma R} \tag{10}$$

$$\frac{dV_2}{dI_2} = \frac{R_2(R_1 + S)}{\Sigma R} \tag{11}$$

$$\frac{dV_1'}{dI_2} = \frac{R_1 R_2}{\Sigma R} \tag{12}$$

Thus, the calculations on the basis of the equivalent circuit of Fig. 12 predict that the slope of V_2' at the origin (Fig. 11, left) should equal that of V_1' (Fig. 11, right). The four slopes determined from each of six experiments, including that of Fig. 11, are shown in Table III. While dV_1/dI_1 and dV_2/dI_2 varied almost two fold, the values of the other two coefficients were very close, in good agreement with prediction. This fact indicates that the equivalent circuit of Fig. 12 is adequate for the present analysis.

In each experiment taking $R_1R_2/\Sigma R$ as the average of the values in columns 3 and 4 of Table III, R_1, R_2, and S were calculated by substitution into Equations 9 and 11. These calculated values are shown in columns 5 to 8 of Table III.

There was somewhat more than a twofold variation in the values of R_1 and R_2 obtained for the different preparations. This range is not unduly

TABLE III

	Slopes					Membrane resistance $10^6\Omega$		
	1 $\frac{dV_1}{dI_1}$	2 $\frac{dV_2}{dI_2}$	3 $\frac{dV'_2}{dI_1}$	4 $\frac{dV'_1}{dI_2}$	5 Average of columns 3 and 4	6 R_1	7 R_2	8 S
I	1.48	1.18	0.43	0.43	0.43	2.1	1.5	3.6
II	0.90	1.31	0.35	0.39	0.37	1.1	2.0	2.9
III	1.53	1.30	0.65	0.68	0.67	2.5	1.8	2.3
IV	1.26	0.70	0.19	0.21	0.20	1.5	0.8	3.7
V	0.83	0.68	0.24	0.22	0.23	1.1	0.9	2.2
VI	0.84	1.02	0.24	0.27	0.25	1.4	1.9	4.2

large in comparison with resistance measurements on other cells or the values obtained from the lateral giant axons by conventional methods (Table I). In addition to the usual biological variation it is also likely that damage was produced by inserting four microelectrodes into a small region of axon. Since the septal membranes were intact the variation in their resistance due to this experimental factor was absent and this may account for the smaller spread of the values calculated for S (Table III).

Another test for the validity of the equivalent circuit of Fig. 12 is shown in Fig. 13, from an experiment on fiber I of Table III. The intracellular potential on one side of the septum was set by an appropriate current. The voltage on the other side was then made the same, within 1 mv, by adjusting the current on that side. Since the voltage drop across S was then zero, $V_1 = I_1R_1$ and $V_2 = I_2R_2$. The agreement between the data and the slopes of the lines drawn from the calculated values of R_1 and R_2 (Table III) is quite satisfactory, and lends further support for the equivalent circuit of Fig. 12. It may be noted

that in Fig. 13 deviation from the linear voltage-current relations occurred at a depolarization of about 5 mv and at hyperpolarization of about 20 mv.

CURRENT-VOLTAGE RELATION OF THE SEPTUM The equivalent circuit of Fig. 12 was also used to obtain the current-voltage relation across the septum from the data of Figs. 11 and 13. For current I_1

$$V_s = V_1 - V_2'$$

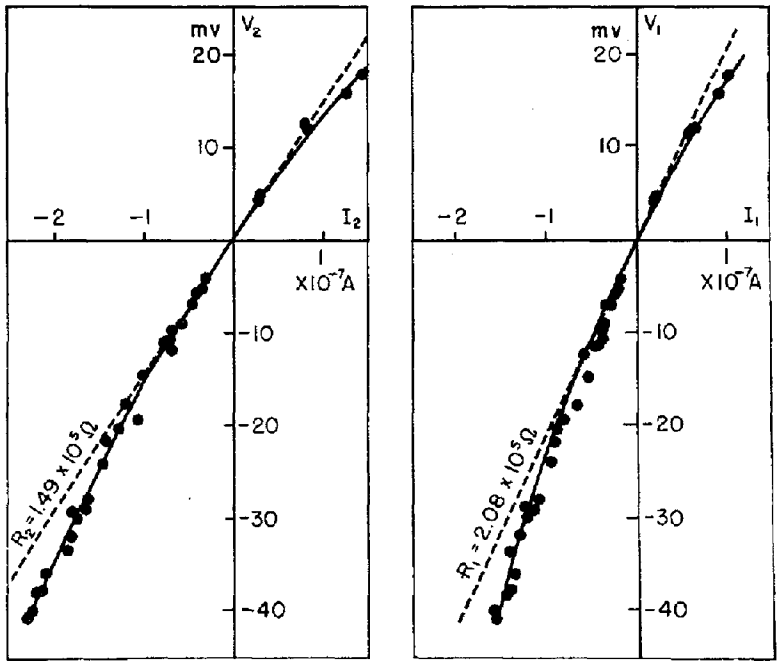

FIGURE 13. Voltage-current relations across R_1 (*right*) and R_2 (*left*) when the potential across S was maintained at zero. The broken lines are the gradients calculated from the data of Fig. 11 (*cf.* also Table III) on the basis of the equivalent circuit of Fig. 12.

However, the values of V_2 in Fig. 13 (left) which correspond to V_2' of Fig. 11 (left) were produced by currents through I_2 that were equal to i_1', the current through the septum in the experiment of Fig. 11 (left). In Fig. 14 these values are plotted as I_s *vs.* V_s (filled circles). Another set of I_s–V_s pairings, but for current flow through S in the opposite direction, was obtained by the same procedure, from the data of Figs. 11 and 13 (right). They are plotted as the open circles of Fig. 14, in which the line has been drawn from the calculated value of S for fiber I in Table III.

The match between the different sets of data which is evidenced in Fig. 14 is remarkably good. It leads to the conclusion that the equivalent circuit

adopted (Fig. 12) is, indeed, adequate for the present experimental conditions, and that calculation of S (Table III, Fig. 14) using that circuit gives reliable values. Although the current-voltage relation of Fig. 14 does not cover a very wide range it is nevertheless possible to conclude that for values of $\pm$ 25 mv change in V_s there is no appreciable deviation from linearity. This is in sharp contrast to the findings on the junction between the lateral giant and motor giant fibers (29). The deviations, which began at lower values of

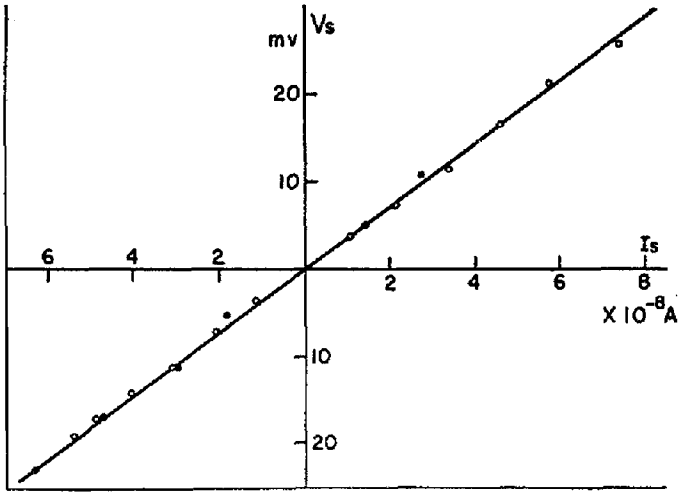

FIGURE 14. The current-voltage relation of the septal membranes. Calculations from the experiments of Figs. 11 and 13 (*left*) plotted as filled circles and of Figs. 11 and 13 (*right*) as the open circles. The line is the value of S for fiber I taken from Table III. Description in text.

membrane polarization in Figs. 11 and 13, presumably resulted from reactions of the axonal membranes (39), not those of the septum.

D. *Nature of Septal Transmission*

EFFECTS OF THE MEMBRANE POTENTIAL OF THE POST-SEPTAL SEGMENT

With the validity of the equivalent circuit of Fig. 12 established, analysis is now possible of the data of experiments such as those of Figs. 7 to 9. During hyperpolarization of the post-septal segment there were three stages noted in the change of the post-septal response: (*a*) Delay and disappearance of the spike, leaving behind a post-septal potential. (*b*) Diminution in the amplitude of the latter. (*c*) Subsequent increase of the pure septal potential linearly with the post-septal hyperpolarization.

Qualitatively this behavior resembles that noted in the case of the post-junctional potential of the squid giant axon junction (45), which appears to

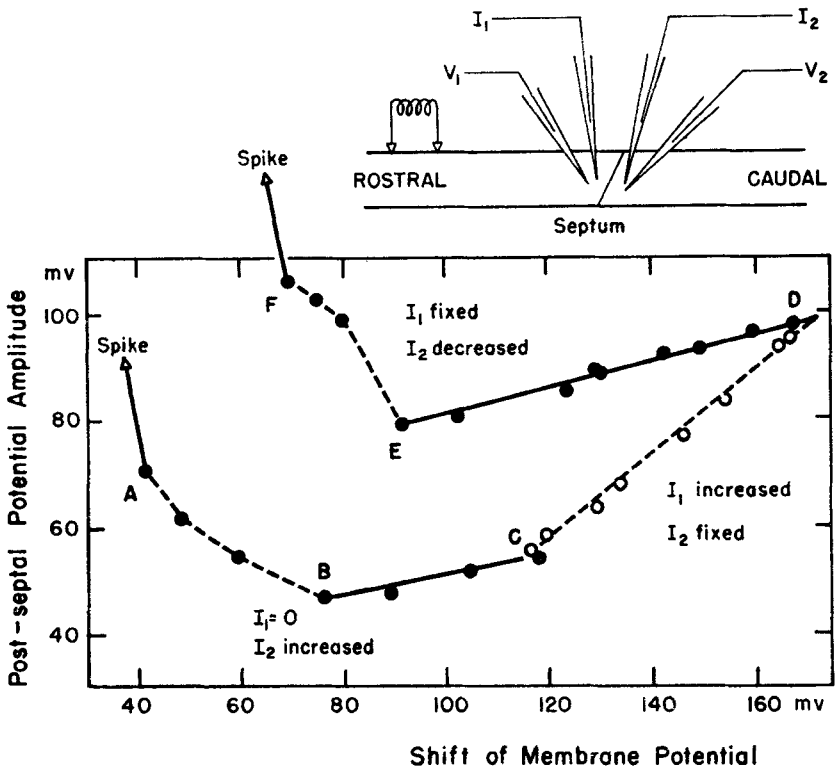

FIGURE 15. Relation between the amplitude of the septal potential and the membrane potential of the post-septal segment. The diagram shows the experimental arrangement. I_1 and I_2, electrodes for applying current; V_1 and V_2, voltage-measuring electrodes. Stimulating electrodes rostral on the nerve cord evoked a pre-septal spike which caused a septal potential and a spike in the caudad segment. The graph shows the changes in the septal potential as the caudal segment was hyperpolarized. The abscissa is the increase of internal negativity above the resting potential. Note that the origin of the graph is not shown. *Filled circles*, the potential of V_2 was changed by changing current in I_2. *Open circles*, the potential was changed by increasing I_1. Block of the post-septal spike occurred at *A*. The septal potential decreased until a minimum value (*B*) which was probably that of the "true" septal potential. Further hyperpolarization of the segment by increasing the current in I_2 led to a small rise in the septal potential (*B* to *C*). The rate of rise increased (*C* to *D*) when hyperpolarizing currents of increasing strength were applied through I_1. With the latter current fixed at its maximal value (*D*), the decreased hyperpolarization of the post-segment caused by progressively diminishing I_2 resulted in a decline of the septal potential. The rate of change (*D* to *E*) was like that in the reverse direction in *B* to *C*. The minimum septal potential (*E*) was much larger than at *B* and occurred at a different membrane potential. With a small further decrease in I_2 the septal potential evoked a local response (*E* to *F*) and the spike reappeared at *F*.

be an electrically inexcitable, postsynaptic potential (34, 36). However, extrapolations of the lines in Fig. 8 cross the zero of the ordinate at 96 and 100 mv depolarization; *i.e.*, with the membrane potential inside positive. For depolarizing p.s.p.'s such as that of frog muscle endplate (18, 77), the squid

axon junction (45), and the frog sympathetic neuron (69), the reversal potential is at an inside negative value. The difference, as is shown in Figs. 15 and 16, is due to the fact that the amplitude of the septal potential does not depend directly on the amplitude of the membrane potential in the post-septal segment, but rather on the amplitude of the pre-septal spike; *i.e.*, it is an electrotonic potential.

The experimental arrangement, as well as the data, is shown in Fig. 15. A spike was elicited in the giant axon by a stimulus to the nerve cord. It propagated into the pre- and post-septal segment, to be recorded by microelectrodes V_1 and V_2. The membrane potential on both sides of the septum could be changed by applying currents through electrodes I_1 and I_2.

A spike occurred in the post-septal segment until the latter was hyperpolarized by about 40 mv (A) by increasing the current in I_2 ($I_1 = 0$). The remaining potential continued to decrease in amplitude (as in Fig. 7) presumably because the local response of the post-segment was diminishing. At B the potential in the post-segment probably represented the septal potential. With increasing currents through I_2 the potential increased again. The rate of increase was small, the septal potential rising by about 8 mv for an increase of 40 mv hyperpolarization. The regression line for B to C passes through the abscissa at a membrane potential of about 100 mv *inside positive.* The current through I_2 was now left constant at the maximum value and a hyperpolarizing current was also applied through I_1. The increased negativity which the additional current caused in the post-segment was correlated with a larger increase in the post-septal potential (C to D).

The membrane polarization was then decreased by diminishing the current in I_2, leaving that in I_1 constant. The amplitude of the post-septal potential decreased (D to E) somewhat more steeply than it had increased in B to C. Further decrease of I_2 now caused a rise in the post-septal potential (E to F) due to the initiation of a local response in the post-segment, and eventually a spike developed (F). Thus, the local response and spike reappeared in the post-segment when the membrane potential was much more negative than was necessary to cause block at the beginning of the sequence. The difference lies in the fact that the initial hyperpolarization was caused by applying a current through I_2, and the final by a current through I_1.

RELATION BETWEEN PRE-SEPTAL SPIKE AND SEPTAL POTENTIAL The difference in effects stems from the dependence of the post-septal potential on the pre-septal spike. The points in Fig. 16 represent the amplitude of the septal potential for the segment B–E of the curve of Fig. 15, plotted against the amplitude of the pre-septal spike that was recorded at the same time (as in Fig. 9). Despite the complex form of the curve in Fig. 15, the relation in Fig. 16 was linear and the extrapolation of the regression line passed through a point only 2 mv from the origin. Thus, the amplitude of the post-septal

potential was directly proportional to the amplitude of the pre-septal spike. Accordingly, the post-septal potential appears to be elicited by the local current generated by the pre-septal spike and is therefore an electrotonic or ephaptic potential in the post-segment. A postsynaptic potential, in contrast, is caused by active participation of the postsynaptic membrane and is affected by the potential of the latter (23, 36).

THE SAFETY FACTOR OF SEPTAL TRANSMISSION To trigger a post-septal spike the amplitudes of the septal potentials ranged between 30 and 50 mv. From the slope of the regression line of Fig. 16 it may be calculated that to produce a septal potential of 30 mv required a pre-septal spike greater than

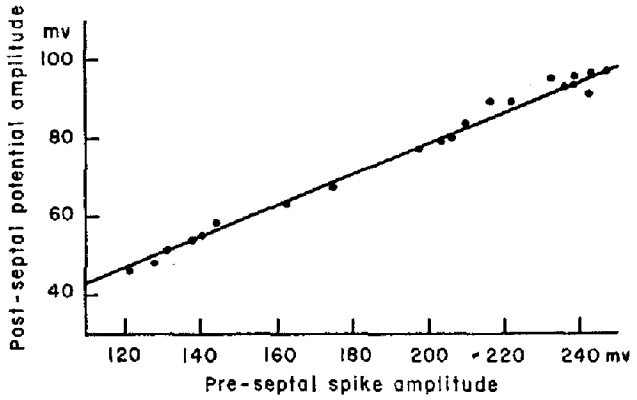

FIGURE 16. Relation between septal potential and pre-septal spike. The amplitudes of the septal potentials in sections *B* to *E* of Fig. 15 are plotted against the amplitudes of the pre-septal spikes that were recorded with microelectrode V_1 during that experiment. The regression line passes within 2 mv of the origin, which is not shown on the scale of this figure.

80 mv and for 50 mv the pre-septal spike had to exceed 125 mv. The amplitudes of the spikes recorded in the present work were 125 to 150 mv only in fibers with high resting potentials. Thus, the safety factor for the ephaptic transmission across the septum is probably relatively low.

The attenuation factor for the spike was calculated and compared with that from an electrotonic potential in five fibers (Table IV). In three of the five, including two in which the attenuation was measured in both directions, there was good agreement between the two values. For the five ratios obtained on these fibers the average was 1.0. In two other fibers the ratio was 1.5 and 1.6 respectively, with attenuation of the applied current being greater. Thus, despite the fact that reactance factors play some role in transmission of the brief pulse generated by a spike while only steady state conditions were measured in the transmission of applied current, the equivalent circuit of

Fig. 12 was nevertheless adequate to account for impulse transmission across the septum. Possible sources of the deviations in Table IV will be discussed below.

In one of the two fibers in which the currents flowing in both directions across the septum were measured, the rostrocaudal attenuation, though the larger for the applied currents, was the smaller for the spikes. The difference, though in the right direction, was not great enough, however, to establish that it might be responsible for the smaller septal delay in rostrocaudal conduction than in caudorostral conduction (Table II). As was noted in connection with Fig. 6, the rostrocaudally produced septal potential had a faster rise, which suggests that the capacities of the membranes of the two ends of the segments may have been somewhat different.

TABLE IV
ATTENUATION FACTORS FOR APPLIED CURRENT (A) AND SPIKES (B)

Fiber No.	Direction of impulse	A	B	A/B
I	r → c	2.7	2.5	1.1
	c → r	2.4	2.7	0.9
II	r → c	1.7	1.9	0.9
	c → r	1.8	2.0	0.9
III	c → r	1.9	1.6	1.2
IV	c → r	3.2	2.2	1.5
V	c → r	3.0	1.9	1.6

E. *Commissural Transmission*[1]

SPREAD OF ELECTROTONIC POTENTIALS When hyperpolarizing currents were applied to one of the lateral giant axons a small potential was also observed in the homologous segment of the other fiber. The ratio between the magnitudes of the applied potential and the potential recorded in the opposite fiber was about 12:1. However, although the potential was small, the possibility of artifact could be excluded. When either recording electrode was withdrawn from the axon that it was impaling, the potential change that it had previously recorded, due to the applied current, disappeared, while that recorded with the remaining electrode was unaffected. Thus, coupling due to a common resistance between the recording microelectrodes and ground could be ruled out, and the spread must have been by electrotonic connections.

The small amount of the electrotonic spread precluded quantitative analysis

[1] Dr. Thomas G. Smith, while a medical student at the College of Physicians and Surgeons, took part in the work illustrated by the experiments of Figs. 18 and 20. We wish to thank him for permitting the use of the data.

of the properties of the commissural ephaptic junction comparable to that which was made for the septal junction. However, the observed ratio of the electrotonic spread is consistent with the conclusion that the junction occurs at the tips of the commissural branches. Electrotonic spread would be attenuated not only because of the distance of the junctional site from the transjunctional recording electrode in the body of the axon, but also because of the electrical circuit conditions imposed by the anatomy.

The two commissural branches are small in diameter in comparison with the axons and they probably also taper to some extent in their distal portions. Thus, the resistance that the branches offer to spread of current must be comparatively high. Furthermore, the small current passing across the ephaptic junction must spread over a large surface in the body of the post-ephaptic axon, and the voltage change on the membrane of the axon must thereby be reduced.

Detailed study of the commissural junction therefore would require impalement of the fine branches, which probably would have to be carried out without visual control. Nevertheless, the fact that the commissural junction can transmit activity from one axon to the other (Figs. 4, 17–20) provides some information about the system. It is most likely that when transmission occurs both commissural branches generate spikes. If the critical firing level at the ephaptic junction is like that at the septum the junctional membranes of the commissural branches probably would have about the same resistance as do the septal membranes. Otherwise the junction would be relatively ineffective since even the septal junctions operate with a low safety factor.

BIDIRECTIONAL TRANSMISSION Functional connections between the commissural branches of one segment permitting transfer of activity in either direction were demonstrated with experiments like that shown in Fig. 17 and analogous to those of Rushton (74) with external recordings for the earthworm. Stimuli were applied to both ends of the nerve cord, but conduction into the segment from the rostral direction was blocked in one axon and from the caudal side in the other axon. A recording microelectrode was inserted into each axon just rostrad to the septum, and in one axon (the left of the experiment of Fig. 17, and the lower fiber in the diagram), a second electrode was inserted for applying currents.

As was described in connection with Fig. 3, the pre-septal spike elicited in the left axon by a rostral stimulus (the earlier spike in Fig. 17*A'*) had a smooth form. A similar, but delayed spike was recorded from the right axon and must have arisen by transfer of excitation across the commissural junction. That the transfer is bidirectional was shown by the responses of both axons on stimulating the caudal part of the nerve cord (*B'*). The spike of the right axon occurred first, but it was now of the post-septal type, with a pronounced

septal potential initiating the segmental spike. The spike of the left axon could only have arisen by transfer across the commissural junction and in its response there is clearly seen a small commissural potential in tempo with

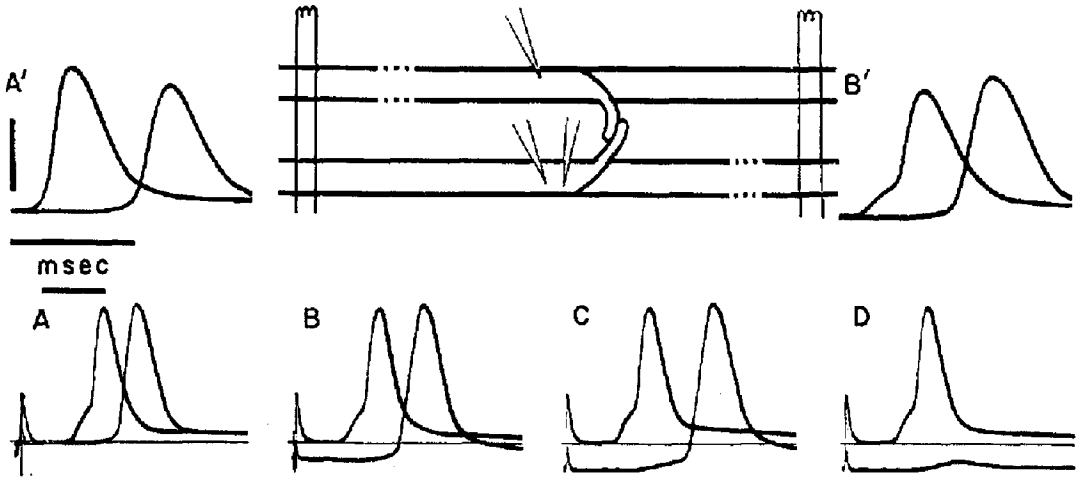

FIGURE 17. Bidirectional transmission at a commissural junction. The two axons are shown diagrammatically in the upper row, as seen from above, rostrad on the left. Two pairs of external stimulating electrodes were applied to the nerve cord respectively, rostrad to an interruption of the right axon and caudad to section of the left axon. The two injuries are shown by interrupted lines. Recording microelectrodes were inserted rostrad to the septum in each axon and a second electrode was also inserted for applying polarizing currents to the left axon. *A'*, responses of the two axons to stimulation of the rostral nerve cord. The first spike is that conducted in the left axon; the delayed second spike is that of the right axon after transmission across the commissural junction. The smaller amplitude of this spike reflects the injury of the rostrad portion of the segment. *B'*, responses recorded on stimulating the nerve cord through the caudal electrodes. The initial spike is now that of the right axon, arising on a septal potential. The long septal delay is a further indication of the decreased excitability of the cut segment. The second spike is that of the left axon after transmission across the commissural junction. While the peaks of the two spikes were closer together in *B'* than in *A'*, the interval between the start of the septal potential and the transcommissural spike in *B'* was the same as that between the starts of the two spikes in *A'*. *A–D*, a sequence of records as in *B'*, but at half the sweep speed, and with application of progressively increasing hyperpolarizing currents to delay and block the transcommissural spike of the left axon. The small commissural potential was then revealed.

the spike of the right axon. On applying hyperpolarizing currents to the left axon the spike of the latter was progressively delayed (*B*, *C*) and finally blocked (*D*). The small commissural potential remained.

UNIDIRECTIONAL TRANSMISSION Frequently commissural transmission at a particular segmental level was only unidirectional. The experimental arrangement of Fig. 18 was the same as that for the experiment of Fig. 17,

except that the axons were intact, and a stimulus to the nerve cord excited both axons directly (*C*). The conduction velocity was slightly higher in the axon recorded on the upper traces, which was also the one impaled with a stimulating microelectrode. When an intracellular depolarization evoked a spike in this axon (*B*) the other axon did not respond, but a small commissural

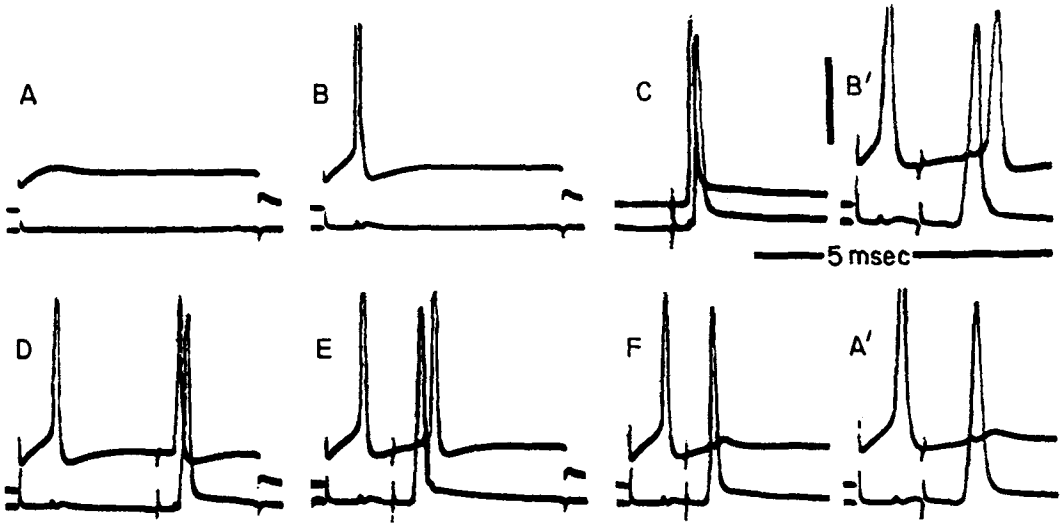

FIGURE 18. Unmasking of a unidirection commissural junction. Experimental arrangement as in Fig. 17, except that the axons were intact. Recording from the left axon on upper trace. *A*, weak intracellularly applied depolarizing stimulus to the left axon caused a local response. *B*, when a stronger stimulus evoked a spike there was a brief capacitative artifact in the other axon followed by a longer lasting but small commissural potential which did not produce a transmitted spike. *C*, the two axons responded to an external stimulation of the nerve cord, the left axon somewhat earlier than the right. *D*, the same timing was maintained when the cord stimulus was delivered about 8 msec. after a spike was evoked in the left axon by intracellular stimulation. *E*, at an interval of about 2.5 msec. the cord stimulus evoked a spike only in the right axon. A response occurred later in the left axon due to commissural transmission. *F*, the commissural potential in the left axon remained when transmission was blocked during refractoriness. *A'*: the same stage is shown at a high sweep speed. *B'*, a stronger depolarization of the left axon elicited its spike earlier. The spike of the right axon was now capable of eliciting a smaller transmitted spike in the left axon. The spikes in this and two subsequent figures have been retouched. 5 msec. calibration on left applies to records *A–F*.

potential did develop. A stimulus to the nerve cord, applied during the relatively refractory period of the directly excited axon (*E*) now caused a reversed sequence of the responses in the two axons. The later response of the axon that had also been excited intracellularly arose by commissural transmission. When the stimulus to the nerve cord was delivered still earlier after the intracellular stimulus (*F*) transmission failed and a commissural

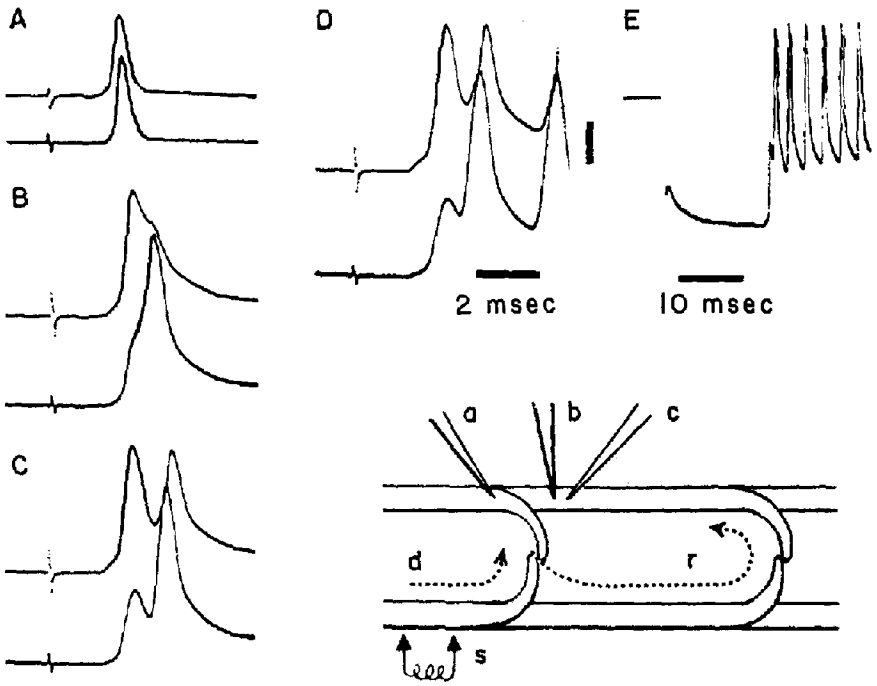

FIGURE 19. Unmasking of a reverberatory loop. Diagram shows experimental arrangement: **a,** recording microelectrode in rostrad segment of right axon; **b, c,** recording and polarizing electrodes in caudad segment; **s,** stimulating electrodes to rostral nerve and delivering a weak shock which excited only the left axon. *A,* responses in the right axon after transmission across the commissure by pathway **d** of the diagram. Upper trace in records *A–D* is from electrode **a,** *B–D,* effects of applying increasing hyperpolarizing currents. Absolute changes in membrane potential not shown. Both segments were hyperpolarized, but the caudad more, as denoted by the increased responses of the two segments. The effects of the hyperpolarizations are described in text. *E,* only the trace registering from electrode **b** is recorded, at the same amplification but at a slower sweep speed. The initial resting potential and the amount of hyperpolarization are shown. About 12 msec. after the hyperpolarization was instituted the stimulus to the cord was applied. The initial deflections are the commissural and septal potentials as shown in detail in the lower trace of *D.* Six responses at 400/sec. of a train that was probably initiated through loop **r** of the diagram are shown.

potential of considerable amplitude was then disclosed. The time relations between this potential and the spike in the other axon are shown in more detail in *A′*. When the depolarizing stimulus was made still larger the commissural potential, summating with the depolarization, again evoked a spike (*B′*), but this response, arising during relative refractoriness and in a strongly depolarized axon, was of low amplitude.

REPETITIVE ACTIVITY DUE TO CIRCUITS OF COMMISSURAL JUNCTIONS A single brief stimulus to the nerve cord can elicit a train of spikes in the lateral

axons (37, 57), but the medial giant axons do not respond repetitively. Occasionally, when small axons of the nerve cord were impaled in the course of the present work, brief stimuli evoked repetitive spikes in these fibers, and their activity might therefore give rise to the synaptic bombardment often seen in the lateral giant axons (57, 58).

However, as surmised in the earlier work, production of trains of repetitive activity at frequencies as high as 400/sec. after a single brief stimulus may involve the commissural interconnections of the two lateral axons. The data of Figs. 19 and 20 analyze this type of repetitive activity.

The right giant axon was impaled in the experiment of Fig. 19 (as in the

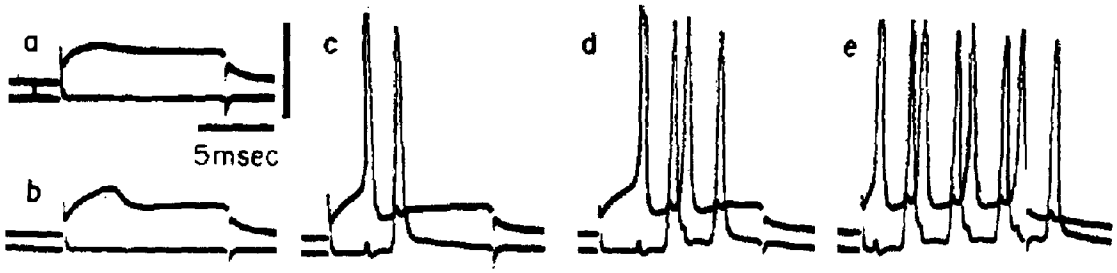

FIGURE 20. Repetitive activity due to reverberation between the two lateral giant axons. Three microelectrodes as in the diagram of Fig. 17, but with the two axons intact. Simultaneous recording from both axons of responses evoked by stimulation of the left axon by intracellular depolarizations of increasing strengths. The trace representing the activity of the right axon was lowered to simplify the registrations. *a*, *b*, the stimuli to the left axon produced only graded local responses without affecting the right axon. *c*, when a spike was evoked in the left axon a response was also obtained in the right. A small artifact due to capacitative cross-coupling was produced in each trace by the spike of the other axon. *d*, *e*, stronger depolarization produced one pair and three pairs of repetitions, respectively. Further description in text.

diagram). A weak stimulus to the rostral nerve cord excited only the other (left) axon and the responses recorded in the two impaled segments of the right axon were elicited *via* commissural transmission. The pre-septal spike (*A*, *upper trace*, recorded with microelectrode a) had a marked commissural component. The post-septal spike (*lower trace*, recorded with microelectrode b) arose with only brief septal delay and the notch on the rising phase is not prominent. The axon was then hyperpolarized with progressively increasing currents applied through microelectrode c.

The initial effect (*B*) was to delay the spike of the rostrad segment on the commissural potential and to increase its amplitude, as described in the preceding part. The septal potential recorded in the caudad segment also increased as described above, and gave rise to a large spike in the strongly hyperpolarized caudad segment. The delay in the post-septal spike permitted

appearance of a septal potential on the falling phase of the spike of the rostrad segment.

Further hyperpolarization of the caudad segment (*C*) led to a spike in the latter which arose well after the septal potential had begun to fall. Thus, the delayed caudad spike was not initiated by the septal potential; instead, it must have been initiated at a more caudad site, propagating rostrad into the recording region. Rostrad propagation continued across the septum, and the second spike of the rostrad segment arose high on the falling phase of the preceding spike, but about half of its potential was probably contributed by the septal component due to electrotonic spread of the preceding large caudad spike.

Still stronger hyperpolarization of the caudad segment did not cause further delay of the spike (*D*). A second response developed in this segment which was also followed by a spike in the rostrad segment. At a slower sweep speed, and recording only from the caudad segment (*E*) the response to the single brief shock to the nerve cord is seen to have been a train of spikes at 400/sec.

Although recording from the other axon was not available the sequence of events could be analyzed with a considerable degree of certainty and the conclusions could be confirmed in other experiments, such as that of Fig. 20, which will be described later. The weak stimulus to the rostral nerve cord caused transmission from the left axon to the right over the commissural pathway **d**. In the unpolarized axon conduction then proceeded caudad with transmission across the septum. On block of the transmission in the hyperpolarized axon transmission at a second commissural junction (**r**), probably that of the caudad segment, initiated a spike at the base of the caudad segment. This spike, now propagating rostrad and probably more slowly than normally, since the axon was hyperpolarized, arrived at the septum late enough to cause ephaptic reexcitation of the rostrad segment. The left axon was now reexcited, either by reversed transmission at **d**, or by transmission at a more rostral commissural junction. Caudad propagation in the left axon again engaged transmission at junction **r** and the cycle was again started.

This sequence is confirmed and further data are added by the experiment of Fig. 20. The experimental arrangement was as in the diagram of Fig. 17, except that as in the experiment of Fig. 18 both axons were intact. Also as in Fig. 18, the current electrode inserted in one axon (left, and registering on the upper beam) was used to depolarize the fiber. The intracellularly evoked response of this axon (Fig. 20*c*) evoked a spike in the other axon (right, and lower beam), after a delay of 1.7 msec. Transmissional delay at a commissural junction probably does not exceed 0.8 msec. (Figs. 17, 18). Thus, the intracellularly evoked spikes must have propagated along the right axon for some

0.4 to 0.5 msec. before crossing to the left axon and invading the recording site of the latter. Since the average conduction velocity is about 10 m/sec. the conduction path might have been 5 mm long, and thus about the length of one abdominal segment in the preparations employed.

When the current was increased a second spike was produced in the depolarized axon (*d*). At an interval of 1.7 msec. the other axon also developed a spike. The number of repetitions increased (*e*) when a still stronger depolarizing current was applied. The frequency of the discharge in both axons was about 400/sec., as it was also in the axon of Fig. 19. It was also a commonly observed rate of repetitive discharge in axons of earlier work (37, 57).

The patterns of the repetitive activity in the two axons of Fig. 20 indicate the mode of origin of the responses, as reverberations between the two axons. They also indicate the approximate sites at which the spikes in the two axons were initiated. The interval between the intracellularly evoked spike of the right axon and the response of the left was 1.7 msec., too long for transmission across the commissural junction of the segment. This commissural junction apparently had low transmissional potency and, as described above, transmission of the spike evoked in the right axon probably occurred at the commissure of the next segment. However, when the right axon was depolarized strongly its excitability must have been increased. The spike of the left axon could now initiate a second spike in the right fiber. The transmissional delay was about 0.9 msec. and the interval between the two spikes of the right axons accordingly was about 2.6 msec. The second spike in turn initiated a spike in the left axon, again over the more distant commissural junction. Increasing the excitability of the right axon by stronger depolarization (*e*) led to a second and third reverberation in the two axons, around the loop r that is shown in the diagram of Fig. 19. The timing of the spikes in the two axons of Fig. 20 has a remarkably steady pattern. This and the repetitive discharge at a rate observed very commonly in other experiments indicate that the loop is stable and that it is relatively simple, as might be expected from the components postulated in Fig. 19.

Thus it is likely that similar reverberations, due to cross-excitation in the commissural cross-couplings, though perhaps elicited against a background of synaptic bombardment, are also responsible for most of the repetitive activity observed in the lateral giant axons after a brief stimulus to the nerve cord. In these trains, the responses after the first usually originated at sites other than that which was stimulated (37).

DISCUSSION

NATURE OF SEPTAL TRANSMISSION The data presented above lead to the conclusion that transmission across the septa in the lateral giant axons of crayfish is ephaptic, by the local circuit current generated during the action

potential of the pre-septal segment. The septal membrane appears to be a passive resistive component permitting current flow equally in either direction. Transmission accordingly is unpolarized, although perhaps it is more readily achieved in one direction than in the other. Due to the resistance of the septal membranes a short, but finite delay occurs in the initiation of the post-septal spike, but the electrotonic septal potential from which the latter arises begins simultaneously with the pre-septal spike. The amplitude of the septal potential depends directly on the amplitude of the pre-septal spike, and is independent of the membrane potential of the post-septal segment, except in so far as the latter affects the amplitude of the pre-septal spike. The septal membranes may be represented quantitatively in a simple equivalent circuit in which the septum is a coupling resistance between the resistances of the pre- and post-septal segments.

The discrepancy between the effectiveness of septal transmission for pulses of applied currents and spikes in some experiments (Table IV) might have been caused by one of several factors: (*a*) The septal membranes might have rectifier properties for large depolarizing voltages, such as are produced at the peak of the spike. (*b*) The membranes might have a parallel capacity which would permit the pulse of the spike to develop a larger septal potential than would be expected from the steady-state measurement with applied currents. (*c*) The spike amplitude recorded by the microelectrode might be somewhat smaller, because of damage, than the spike at sites immediately adjacent to the septum.

Preliminary experiments with voltage clamp methods (*cf.* references 46, 51) do not support the first two alternatives. These results indicate that the I_s–V_s relation (*cf.* Fig. 14) is linear over a range of more than 70 mv. When the potential on one side of the septum was changed by step functions, the potential on the other side changed monotonically, without an initial peak. Accordingly, we incline toward adoption of the third alternative explanation. An indication in favor of this possibility is seen in the experiment of Fig. 17. There was marked delay of the post-septal spike for caudorostral transmission, but the interval between the septal potential and the post-commissural spike was identical in both directions. Probably the damage caused in the rostrad segment by its division caused delay of septal transmission, as recorded at the microelectrode site, but transmission into the commissural branch must have been unaffected.[2]

[2] The anatomical asymmetry due to the presence of a commissural branch on the rostrad side of this septum might itself account for the lesser delay in rostrocaudal transmission. The branch always seems to develop a spike when the segment from which it arises has discharged, since a commissural potential is then always found in the other axon. Thus, in rostrocaudal conduction the current "sink" of the active pre-septal area is probably larger than the sink for current flow in the opposite direction which is associated with caudorostral transmission.

The various properties of septal transmission clearly define the difference between the ephaptic nature of the transmission and that of synaptic transmission. Electrical inexcitability of the synaptic membrane and minimal electrotonic spread from the activity of the presynaptic nerve terminals combine in the latter, so that chemical transmission by the release of a transmitter agent from the terminals appears to be obligatory (34, 36, 40, 41).

VARIETIES OF EPHAPTIC JUNCTIONS Anatomical contacts that are physiologically defined as ephaptic junctions occur in a number of situations and may be classified on the basis of the tightness of coupling between the pre- and post-ephaptic units. Tight coupling is evidenced in those cases in which electrotonic spread from a pre-spike produces enough depolarization in the post-unit to elicit a spike. This is clearly the case in the septal junctions of crayfish and earthworm; in the lateral giant–motor giant junction of crayfish; and probably also at the junctions between the commissural branches of the lateral giant axons in crayfish. The intercalated discs of cardiac muscle (*cf.* reference 75) may also be classed among tightly coupled ephaptic connections.

Looser couplings, but occasionally strong enough to evoke spikes of the post-units, probably account for the "quasi-artificial synapses" of various polychaetes (16), and perhaps also are responsible for the dorsal root reflex which occurs in the spinal cord of mammals (78) and fish (9). Still looser couplings in which the pre-spike exerts only modulating effects on the post-units are demonstrable between neurons of lobster cardiac ganglion (46, 81, 82), between supramedullary neurons of fish (6, 7), and between muscle fibers of decapod crustaceans (72).

There is probably a ladder-like network of interconnections between the giant axons of annelids (16, 74). If the transmissional potency of these junctions is low, as is sometimes the case in the commissural junctions of the crayfish lateral giant axons, transmission from one axon to the other in the annelids might be influenced by local conditions at one site or another. Thus, facilitatory effects might be contributed by synaptic bombardments at one segmental level or another and would give rise to shifting sites of transmission at the quasi-artificial synapses (16).

Anatomically distinct interconnections between spinal interneurons and dorsal root terminals have never been described and if ephaptic transmission is responsible for the dorsal root reflex it is probably effected (36) by "field" currents (31, 32), generated by contiguous synaptically activated neurons, and penetrating the terminals to excite the latter electrically. Excitatory and inhibitory field effects accounted for in tempo and sign by the flow of action currents are observed between contiguous axons (60, 63, 66, 70) and in the spinal cord (4, 42). An inhibitory phenomenon observed in Mauthner cells (28) is probably also ascribable to field effects. However, in special experi-

mental conditions transmission of spikes at "artificial junctions" may also occur (3, 49, 71).

While some commissural junctions of the crayfish giant axons may have greater transmissional potency in one direction than in the other, this difference is probably only quantitative (Fig. 18) and akin to the small difference in transmission in the two directions at the septal junctions. Facultative unidirectional ephaptic transmission is known only in the case of the lateral giant to motor giant junction of crayfish (29). The difference between this system and the bidirectional (or potentially bidirectional) ephaptic junctions is formally accounted for by the inclusion of a rectifier in the coupling element of the equivalent circuit of the former (29, 36). From a biophysical standpoint this formalism represents an interesting difference in membrane properties of the septal and the cord-motor giant fiber junctions.

PROPERTIES OF SEPTAL MEMBRANES The septal membranes of the crayfish lateral giant axon appear to be electrically inexcitable. They do not respond electrogenically when large differences of potential are imposed. Furthermore, the voltage-current relation is linear, at least over a range of $\pm$ 25 mv change, while the axonal membrane begins to show non-linearity at depolarizations of 5 mv. Electrical properties like those of the septal membranes are also found in the electrically inexcitable synaptically electrogenic, and in electrogenically inert membranes (10, 11, 13, 39–41). However, the available data do not provide a decision as to whether the septal membranes might respond electrogenically to chemical or other types of stimuli, as do postsynaptic and some receptor membranes (34, 36, 38) or whether they are electrogenically inert, as are the uninnervated membranes of electroplaques of eel (1, 61), some other Gymnotids (*cf.* reference 8), and *Torpedo nobiliana* (13).

RECTIFICATION AT EPHAPTIC JUNCTION OF CORD-MOTOR GIANT FIBERS While the apposed membranes of the lateral giant–motor giant junctions do not generate spikes it is nevertheless incorrect to regard them as electrically inexcitable, as had been done previously by one of us (36) and by Furshpan and Potter (29). Rectification, though it was first observed in spike-generating membrane (*cf.* references 20, 50), nevertheless can also be elicited in cells which do not produce spikes, such as the slow muscle fibers of frog (5, 17, 62), *Raia* electroplaques (8, 12, 19), and some muscle fibers of crayfish (26). The rectification is due to an electrically excited increase in membrane conductance, probably for K^+ in frog slow muscle fibers (5), and for Cl^- in *Raia* electroplaques (19, 39). In the electroplaques the rectification is not associated with a marked electrogenesis except under special experimental conditions (8, 19). The rectification occurs with some time delay in these tissues, whereas it appears to develop rapidly in the junction (29). However, this difference

may be accounted for perhaps by the known diversity in kinetics of electrically excitable processes (39).

At any rate, in a strict sense one or both of the junctional membranes in the lateral-motor giant system must be regarded as electrically excitable. The fundamental nature of the rectifying property may lie either in rectification by the pre-junctional membrane or in anomalous rectification (39) of the post-junctional membrane. It is also possible that both effects might cooperate to account for the very high degree of rectification at the junction.

VARIETIES OF EPHAPTIC MEMBRANES Thus, ephaptic junctions may have electrically excitable (but not spike-generating) membrane, or the latter may be electrically inexcitable. The second variety may include membranes which are electrogenically inert, or some that respond to specific stimuli, as do synaptic and sensory membranes. Since present day morphological techniques cannot distinguish these different varieties (35, 67) the characterization of the system in each specific case must be made by functional tests.

It has been suggested (*cf.* reference 25) that ephaptic systems differ from synaptic in the tighter coupling between the pre- and post-junctional membranes of ephapses. Looseness of resistive coupling, by shunting in the synaptic space, would account for the remarkably small electrotonic pickup in a postsynaptic cell of the activity of the presynaptic terminals (23, 36, 41). The view that some ephaptic junctions have closely abutting membrane with little or no intervening extracellular space and therefore have tight coupling is attractive. However, the degree of coupling can only be a secondary differentiation because (*a*) the postsynaptic membrane does not respond electrogenically to large changes of membrane potential which are derived from extrinsic or intrinsic currents (10, 11, 13, 41, 84) and (*b*) there are various degrees of coupling in ephaptic systems.

Furthermore, it is not yet clear to what extent the ephaptic junction of crayfish lateral to motor giant axons differs structurally from that of the synapse between squid giant axons (65, 73). Recent work on the septa of crayfish axons (48) indicates that except for small areas of apposition of the two axonal membranes, there may actually be more of a connective tissue barrier at the septa than there is, for example, between presynaptic nerve terminals and electroplaques (67, 80). The rectifying ephaptic junctions between lateral and motor giant axons "may fuse into a single electron-dense zone about 50 A° thick" (65), while the apposed membranes at the septa are spaced about 100 A° apart (48). In the medial to motor giant junctions (73 *a*) occasionally "the overall thickness of the synaptic membrane complex is reduced to well below 150 A°".

In view of the uncertainty which still exists even on the basis of electron microscopic data, the earlier division of opinion based on simpler histological

preparations, that the septate axon systems represent synaptic junctions (53, 76) or that they differ profoundly from such junctions (55) cannot carry much weight. The physiological evidence, however, is decisive. Septal transmission operates through an ephaptic mechanism, not through that which obtains at synaptic junctions.

COMMISSURAL TRANSMISSION In view of the fact that the commissural junctions can be bidirectional and that they pass an electrotonic current, it is likely that they, too, are ephaptic. However, for reasons already given, information as precise as that on the septal junctions could not be obtained for the commissural connections. Thus, although the commissural potential did not increase with hyperpolarization (Figs. 17, 19) as a depolarizing p.s.p. may be expected to do (36), this evidence is not decisive. The commissural potential recorded in the axon is small relative to what must be its true size, since it is capable of initiating a spike somewhere along the commissural branch. Furthermore, transmission is delayed by more than 0.5 msec. and spread of current from one axon to the other is very much attenuated. Thus, hyperpolarizing currents delivered to the axon must have been applied at a long distance from the junction as measured in electrophysiological terms. Therefore, synaptic transmission, though unlikely, cannot be ruled out with the available data.

Since the safety factor for septal transmission is relatively low, the ladder of commissural connections provides a considerable degree of insurance that messages carried by the lateral giant axons will be propagated. However, whether the connections cause repetitive, reverberatory activity in the intact animal is doubtful. Instances of the repetitive responses to a single brief cord stimulus were less frequent in the present work than in earlier experiments (57, 58), but reverberatory effects could be elicited by experimental interference with normal propagation by depolarization (Fig. 20) or hyperpolarization (Fig. 19) or by damaging one of the axons. Furthermore, it seems likely that trains of discharges in the cord at frequencies in the neighborhood of 400/sec. would have strong effects on the animal if they occurred normally in response to afferent impulses, but such consequences have not been reported to our knowledge.

This work was supported in part by grants from the Muscular Dystrophy Associations of America, National Institute of Neurological Diseases and Blindness (B 389-C4 and C5), National Science Foundation (NSF G-5665), and the United Cerebral Palsy Research and Educational Foundation. Part of the costs of laboratory space at the Marine Biological Laboratory was defrayed by a grant from the Marine Biological Laboratory under its O.N.R. contract.

Dr. Watanabe held a Visiting Fellowship in the Department of Neurology under a grant from the United Cerebral Palsy Research and Educational Foundation.

A preliminary account was published in 1960 (83).

Received for publication, May 16, 1961.

REFERENCES

1. ALTAMIRANO, M., COATES, C. W., and GRUNDFEST, H., Mechanisms of direct and neural excitability in electroplaques of electric eel, *J. Gen. Physiol.*, 1955, **38**, 319.
2. AMATNIEK, E., Measurements of bioelectric potentials with microelectrodes and neutralized input capacity amplifier, *I.R.E. Tr. Med. Elec.*, March, 1958, p. 3.
3. ARVANITAKI, A., Effects evoked in an axon by activity of a contiguous one, *J. Neurophysiol.*, 1942, **5**, 89.
4. BARRON, D. H., and MATTHEWS, B. H. C., The interpretation of potential changes in the spinal cord, *J. Physiol.*, 1938, **92**, 276.
5. BELTON, P., and GRUNDFEST, H., The ionic factors in the electrogenesis of the electrically inexcitable and electrically excitable membrane components of frog slow muscle fibers, *Biol. Bull.*, 1961, **121**, 382.
6. BENNETT, M. V. L., Electrical connections between supramedullary neurons, *Fed. Proc.*, 1960, **19**, 298.
7. BENNETT, M. V. L., Comparative electrophysiology of supramedullary neurons, *Biol. Bull.*, 1960, **119**, 303.
8. BENNETT, M. V. L., Modes of operation of electric organs, *Ann. New York Acad. Sc.*, 1961, **94**, 458.
9. BENNETT, M. V. L., CRAIN, S. M., and GRUNDFEST, H., Electrophysiology of supramedullary neurons in *Spheroides maculatus*, I, II, III, *J. Gen. Physiol.*, 1959, **43**, 159, 189, 221.
10. BENNETT, M. V. L., and GRUNDFEST, H., The electrophysiology of electric organs of marine electric fishes. II. The electroplaques of the main and accessory organ of *Narcine brasiliensis*, *J. Gen. Physiol.*, 1961, **44**, 805.
11. BENNETT, M. V. L., and GRUNDFEST, H., The electrophysiology of electric organs of marine electric fishes. III. The electroplaques of the stargazer, *Astroscopus y-graecum*, *J. Gen. Physiol.*, 1961, **44**, 819.
12. BENNETT, M. V. L., and GRUNDFEST, H., Structure and function in Rajid electroplaques, *Fed. Proc.*, 1961, **20**, 339.
13. BENNETT, M. V. L., WURZEL, M., and GRUNDFEST, H., The electrophysiology of electric organs of marine electric fishes. I. Properties of electroplaques of *Torpedo nobiliana*, *J. Gen. Physiol.*, 1961, **44**, 757.
14. BULLOCK, T. H., Functional organization of the giant fiber system of the *Lumbricus*, *J. Neurophysiol.*, 1945, **8**, 55.
15. BULLOCK, T. H., The invertebrate neuron junction, *Cold Spring Harbor Symp. Quant. Biol.*, 1952, **17**, 267.
16. BULLOCK, T. H., Properties of some natural and quasi-artificial synapses in polychaetes, *J. Comp. Neurol.*, 1953, **98**, 37.
17. BURKE, W., and GINSBORG, B. L., The electrical properties of the slow muscle fibre membrane, *J. Physiol.*, 1956, **132**, 586.
18. CASTILLO, J. DEL, and KATZ, B., Biophysical aspects of neuromuscular transmission, *Progr. Biophysics*, 1956, **6**, 121.

19. COHEN, B., BENNETT, M. V. L., and GRUNDFEST, H., Electrically excitable responses in *Raia erinacea* electroplaques, *Fed. Proc.*, 1961, **20**, 339.
20. COLE, K. S., Rectification and inductance in the squid giant axon, *J. Gen. Physiol.*, 1941, **25**, 29.
21. CREED, R. S., DENNY-BROWN, D., ECCLES, J. C., LIDDELL, E. G. T., and SHERRINGTON, C. S., Reflex Activity of the Spinal Cord, Oxford, Clarendon Press, 1932.
22. DALTON, J. C., Effects of external ions on membrane potential of a crayfish giant axon, *J. Gen. Physiol.*, 1959, **42**, 971.
23. ECCLES, J. C., The Physiology of Nerve Cells, Baltimore, The Johns Hopkins Press, 1957.
24. ECCLES, J. C., GRANIT, R., and YOUNG, J. Z., Impulses in the giant nerve fibres of earthworms, *J. Physiol.*, 1932, **77**, 23P.
25. ECCLES, J. C., and JAEGER, J. C., The relationship between the mode of operation and the dimensions of the junctional regions at synapses and motor end-organs, *Proc. Roy. Soc. London, Series B*, 1957, **148**, 38.
26. FATT, P., and GINSBORG, B. L., The ionic requirements for the production of action potentials in crustacean muscle fibres, *J. Physiol.*, 1958, **142**, 516.
27. FATT, P., and KATZ, H., An analysis of the end-plate potential recorded with an intracellular electrode, *J. Physiol.*, 1951, **115**, 320.
28. FURSHPAN, E. J., and FURUKAWA, T., personal communication.
29. FURSHPAN, E. J., and POTTER, D. D., Transmission at the giant motor synapses of the crayfish, *J. Physiol.*, 1959, **145**, 289.
30. FURSHPAN, E. J., and POTTER, D. D., Slow post-synaptic potentials recorded from the giant motor fibre of the crayfish. *J. Physiol.*, 1959, **145**, 326.
31. GRUNDFEST, H., Bioelectric potentials, *Ann. Rev. Physiol.*, 1940, **2**, 213.
32. GRUNDFEST, H., Bioelectric potentials in the nervous system and in muscle, *Ann. Rev. Physiol.*, 1947, **9**, 477.
33. GRUNDFEST, H., Instrument requirements and specifications in bioelectric recording, *Ann. New York Acad. Sc.*, 1955, **60**, 841.
34. GRUNDFEST, H., Electrical inexcitability of synapses and some of its consequences in the central nervous system, *Physiol. Rev.*, 1957, **37**, 337.
35. GRUNDFEST, H., *in* The Biology of Myelin. Progress in Neurobiology, New York, Hoeber-Harper, 1959, **4**, 33.
36. GRUNDFEST, H., Synaptic and ephaptic transmission, *in* Handbook of Physiology, Neurophysiology, I, (J. Field, editor), Washington D. C., American Physiological Society, 1959, 147.
37. GRUNDFEST, H., Evolution of conduction in the nervous system, *in* Evolution of Nervous Control, (Allan D. Bass, editor), Washington, D. C., American Association for the Advancement of Science, 1959, 43.
38. GRUNDFEST, H., Excitation by hyperpolarizing potentials. A general theory of receptor activities, *in* Nervous Inhibition, (E. Florey, editor), London, Pergamon Press, 1961, 326.
39. GRUNDFEST, H., Ionic mechanisms in electrogenesis, *Ann. New York Acad. Sc.*, 1961, **94**, 405.

40. GRUNDFEST, H., General physiology and pharmacology of junctional transmission, *in* Biophysics of Physiological and Pharmacological Actions, (A. M. Shanes, editor), Washington, D. C., American Association for the Advancement of Science, in press.
41. GRUNDFEST, H., and BENNETT, M. V. L., Studies on morphology and electrophysiology of electric organs. I. Electrophysiology of marine electric fishes, *in* Bioelectrogenesis, (C. Chagas and A. Paes de Carvalho, editors), Amsterdam, Elsevier Publishing Company, Inc., 1961, 57.
42. GRUNDFEST, H., and MAGNES, J., Excitability changes in dorsal roots produced by electronic effects from adjacent afferent activity, *Am. J. Physiol.*, 1951, **164**, 502.
43. GRUNDFEST, H., and REUBEN, J. P., Neuromuscular synaptic activity in lobster, *in* Nervous Inhibition, (E. Florey, editor), London, Pergamon Press, 1961, 92.
44. HAGIWARA, S., Synaptic potential in the motor giant axon of the crayfish, *J. Gen. Physiol.*, 1959, **41**, 1119.
45. HAGIWARA, S., and TASAKI, I., A study of the mechanism of impulse transmission across the giant synapse of the squid, *J. Physiol.*, 1958, **143**, 114.
46. HAGIWARA, S., WATANABE, A., and SAITO, N., Potential changes in syncytial neurons of lobster cardiac ganglion, *J. Neurophysiol.*, 1959, **22**, 554.
47. HAMA, K., Some observations on the fine structure of the giant nerve fibers of the earthworm, *Eisenia foetida*, *J. Biophysic. and Biochem. Cytol.*, 1959, **6**, 61.
48. HAMA, K., Some observations on the fine structure of the giant fibers of the crayfishes (*Cambarus virilis* and *C. clarkii*) with special reference to the submicroscopic organization of the synapses, *Anat. Rec.*, in press.
49. HERING, E., Beitrage zur allgemeinen Nerven- und Muskel-physiologie. IX. Ueber Nervenreizung durch dem Nervenström, *Sitzungsber. k. Akad. Wissensch., Math-naturwissensch. Cl., Wien*, 1882, **85**, 237.
50. HODGKIN, A. L., and HUXLEY, A. F., A quantitative description of membrane current and its applications to conduction and excitation in nerve, *J. Physiol.*, 1952, **117**, 500.
51. HODGKIN, A. L., HUXLEY, A. F., and KATZ, B., Measurement of current-voltage relations in the membrane of the giant axon of *Loligo*, *J. Physiol.*, 1952, **117**, 424.
52. HODGKIN, A. L., and RUSHTON, W. A. H., The electrical constants of a crustacean nerve fibre, *Proc. Roy. Soc. London, Series B*, 1946, **133**, 444.
53. HOLMES, W., The giant myelinated nerve fibres of the prawn, *Phil. Tr. Roy. Soc. London, Series B*, 1942, **231**, 293.
54. ISSIDORIDES, M., Ultrastructure of the synapse in the giant axon of the earthworm, *Exp. Cell Research*, 1956, **11**, 423.
55. JOHNSON, G. E., Giant nerve fibers in crustaceans with special reference to *Cambarus* and *Palaemonetes*, *J. Comp. Neurol.*, 1924, **36**, 323.
56. KAMADA, T., and KINOSITA, H., Membrane potential of sea-urchin eggs, *Proc. Imp. Acad. Tokyo*, 1940, **16**, 149.
57. KAO, C. Y., Postsynaptic electrogenesis in septate giant axons. II. Comparison of medial and lateral giant axons of crayfish, *J. Neurophysiol.*, 1960, **23**, 618.
58. KAO, C. Y., and GRUNDFEST, H., Conductile and integrative functions of crayfish giant axons, *Fed. Proc.*, 1956, **15**, 104.

59. KAO, C. Y., and GRUNDFEST, H., Postsynaptic electrogenesis in septate giant axons. I. Earthworm median giant axon, *J. Neurophysiol.*, 1957, **20**, 553.
60. KATZ, B., and SCHMITT, O. H., A note on interaction between nerve fibres, *J. Physiol.*, 1942, **100**, 369.
61. KEYNES, R. D., and MARTINS-FERREIRA, H., Membrane potentials in the electroplates of the electric eel, *J. Physiol.*, 1953, **119**, 315.
62. KUFFLER, S. W., and VAUGHAN-WILLIAMS, E. M., Properties of the "slow" skeletal muscle fibers of the frog, *J. Physiol.*, 1953, **121**, 318.
63. KWASSOW, D. G., and NAUMENKO, A. I., Störungen in der isolierten Leitung der Impulse im durch hypertonische Lösungen und Austrockung alterierten Nervenstamm, *Arch. ges. Physiol.*, 1936, **237**, 576.
64. LORENTE DE NÓ, R., A Study of Nerve Physiology, *Studies from The Rockefeller Institute for Medical Research*, 1947, **131, 132**.
65. DE LORENZO, A. J., Electron microscopy of electrical synapses in the crayfish, *Biol. Bull.*, 1960, **119**, 325.
66. MARRAZZI, A. S., and LORENTE DE NÓ, R., Interaction of neighboring fibers in myelinated nerve, *J. Neurophysiol.*, 1944, **7**, 83.
67. MATHEWSON, R. F., WACHTEL, A., and GRUNDFEST, H., Comparative study of fine structure in electroplaques, *in* Bioelectrogenesis, (C. Chagas and A. Paes de Carvalho, editors), Amsterdam, Elsevier Publishing Company, Inc., 1961, 25.
68. NASTUK, W. L., and HODGKIN, A. L., The electrical activity of single muscle fibers, *J. Cell. and Comp. Physiol.*, 1950, **35**, 39.
69. NISHI, S., and KOKETSU, K., Electrical properties and activities of single sympathetic neurons in frogs, *J. Cell. and Comp. Physiol.*, 1960, **55**, 15.
70. OTANI, T., Ueber eine Art Hemmung und Bahnung in Folge der Wechselbeziehungen der Nervenfasern zueinander, *Japan. J. Med. Sc.*, 1937, **4**, 355.
71. RENSHAW, B., and THERMAN, P. O., Excitation of intraspinal mammalian axons by nerve impulses in adjacent axons, *Am. J. Physiol.*, 1941, **133**, 96.
72. REUBEN, J. P., Electrotonic connections between lobster muscle fibers, *Biol. Bull.*, 1960, **119**, 334.
73. ROBERTSON, J. D., Ultrastructure of two invertebrate synapses, *Proc. Soc. Exp. Biol. and Med.*, 1953, **82**, 219.
73 *a*. ROBERTSON, J. D., Ultrastructure of excitable membranes and the crayfish median-giant synapse, *Ann. New York Acad. Sc.*, 1961, **94**, 339.
74. RUSHTON, W. A. H., Reflex conduction in the giant fibres of the earthworm, *Proc. Roy. Soc. London, Series B*, 1946, **133**, 109.
75. SJÖSTRAND, F. S., and ANDERSSON-CEDERGREN, E., Intercalated discs of heart muscle, *in* The Structure and Function of Muscle, (G. H. Bourne, editor), New York, Academic Press, 1960, **1**, 421.
76. STOUGH, H. B., Giant nerve fibers of the earthworm, *J. Comp. Neurol.*, 1926, **40**, 409.
77. TAKEUCHI, A., and TAKEUCHI, N., On the permeability of end-plate membrane during the action of transmitter, *J. Physiol.*, 1960, **154**, 52.
78. TOENNIES, J. F., Reflex discharge from the spinal cord over the dorsal roots, *J. Neurophysiol.*, 1938, **1**, 378.

79. VAN HARREVELD, A., A physiological solution for fresh water crustaceans, *Proc. Soc. Exp. Biol. and Med.*, 1936, **34**, 428.

80. WACHTEL, A., MATHEWSON, R. F., and GRUNDFEST, H., Electron microscopic and histochemical comparison of the two types of electroplaques of *Narcine brasiliensis*. *J. Biophysic. and Biochem. Cytol.*, 1961, **11**, in press.

81. WATANABE, A., The interaction of electrical activity among neurons of lobster cardiac ganglion, *Japan. J. Physiol.*, 1958, **8**, 305.

82. WATANABE, A., and BULLOCK, T. H., Modulation of activity of one neuron by subthreshold slow potentials in another in lobster cardiac ganglion, *J. Gen. Physiol.*, 1960, **43**, 1031.

83. WATANABE, A., SMITH, T. G., and GRUNDFEST, H., Segmental and crossed ephatic transmission in crayfish lateral giant axons, *Fed. Proc.*, 1960, **19**, 298.

84. WERMAN, R., Electrical inexcitability of the synaptic membrane in the frog skeletal muscle fibre, *Nature*, 1960, **188**, 149.

85. WIERSMA, C. A. G., Giant nerve fiber system of crayfish, a contribution to comparative physiology of synapse, *J. Neurophysiol.*, 1947, **10**, 23.

86. YOUNG, J. Z., Fused neurons and synaptic contacts in the giant nerve fibres of cephalopods, *Phil. Tr. Roy. Soc. London, Series B*, 1939, **229**, 465.